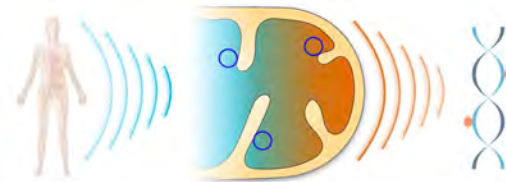


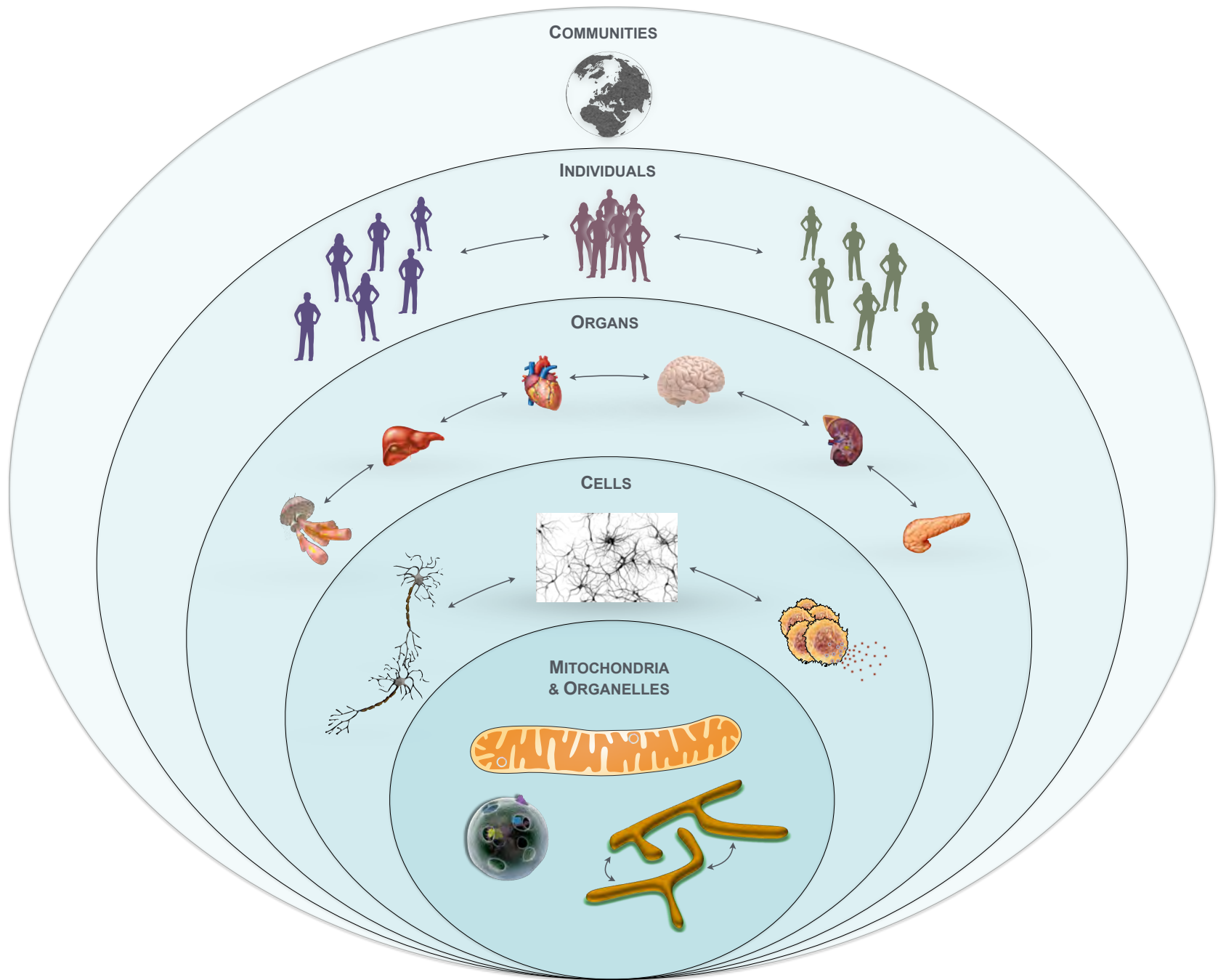
Mitochondrial diversity in mouse and human brains



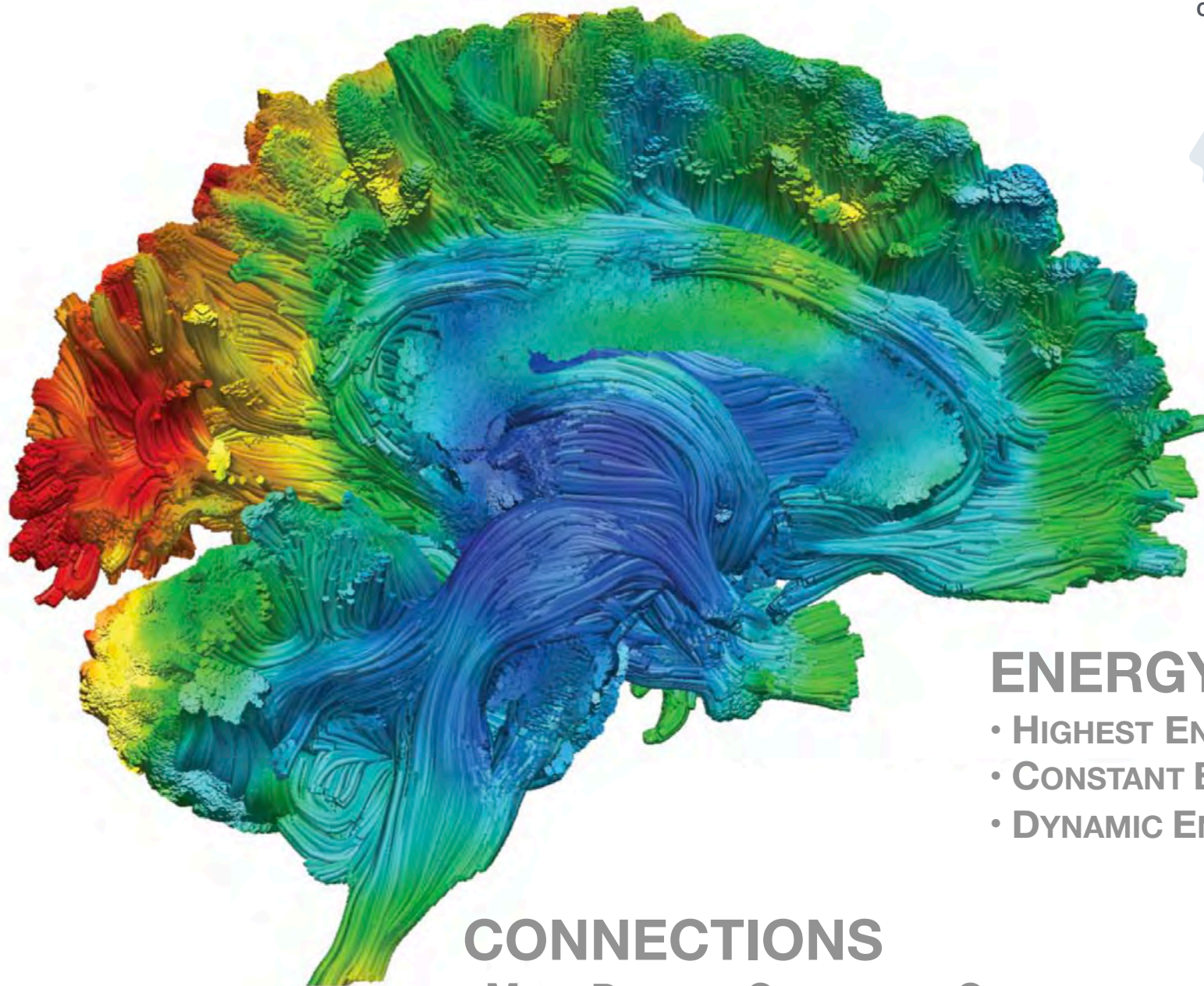
Martin Picard, Ph.D.
Department of Psychiatry, Division of Behavioral Medicine
Department of Neurology, H. Houston Merritt Center
Robert N Butler Columbia Aging Center
Columbia Translational Neuroscience Initiative
New York State Psychiatric Institute (NYSPI)

 **COLUMBIA**
COLUMBIA UNIVERSITY
IRVING MEDICAL CENTER

 **NEW YORK**
STATE OF
OPPORTUNITY. | **New York State**
Psychiatric Institute

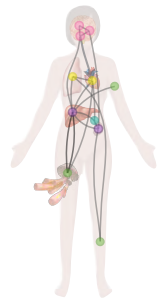
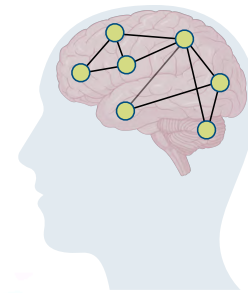


Life is a regulated **energetic cascade** sustained by
information transfer across
interconnected biological systems



Cell network (brain)

Organ network



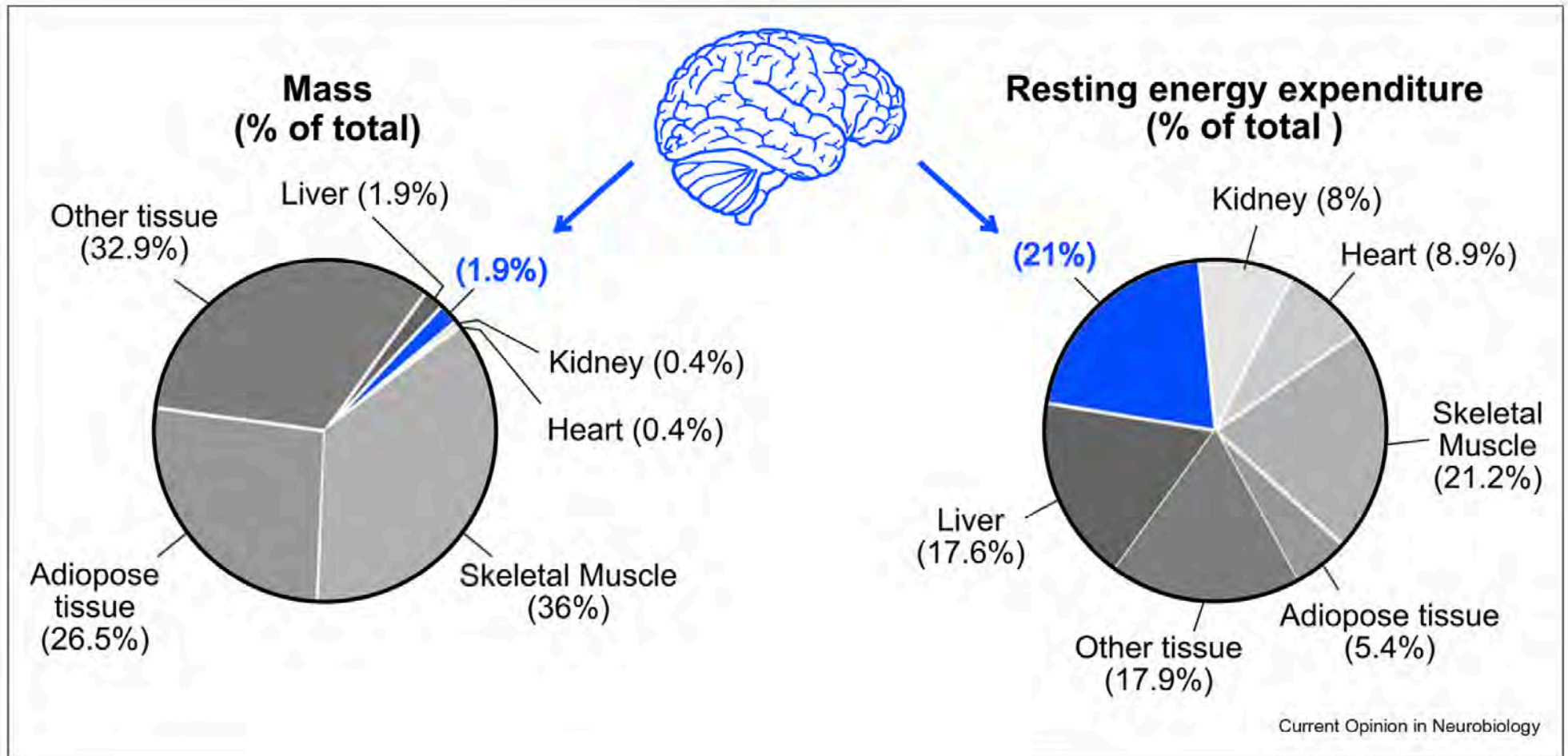
ENERGY

- HIGHEST ENERGY CONSUMPTION
- CONSTANT ENERGY FLUX
- DYNAMIC ENERGY PATTERNS

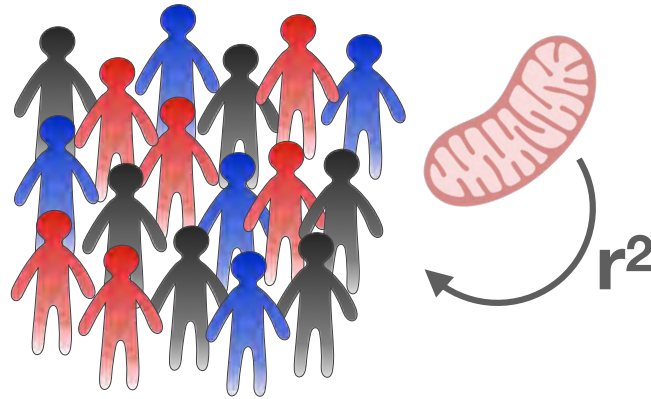
CONNECTIONS

- MOST DENSELY CONNECTED ORGAN
- LONG-RANGE CONNECTIONS
- PLASTICITY

The brain's enormous, constant energy demand

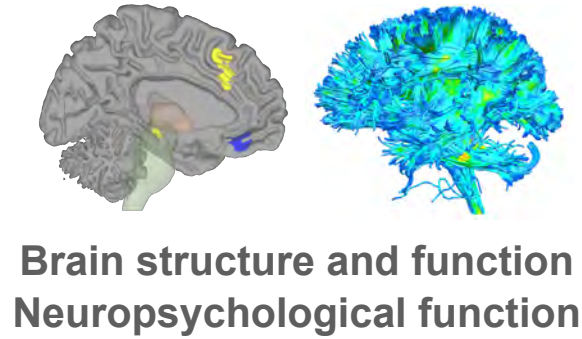


Variations from rest to activity is ~5%

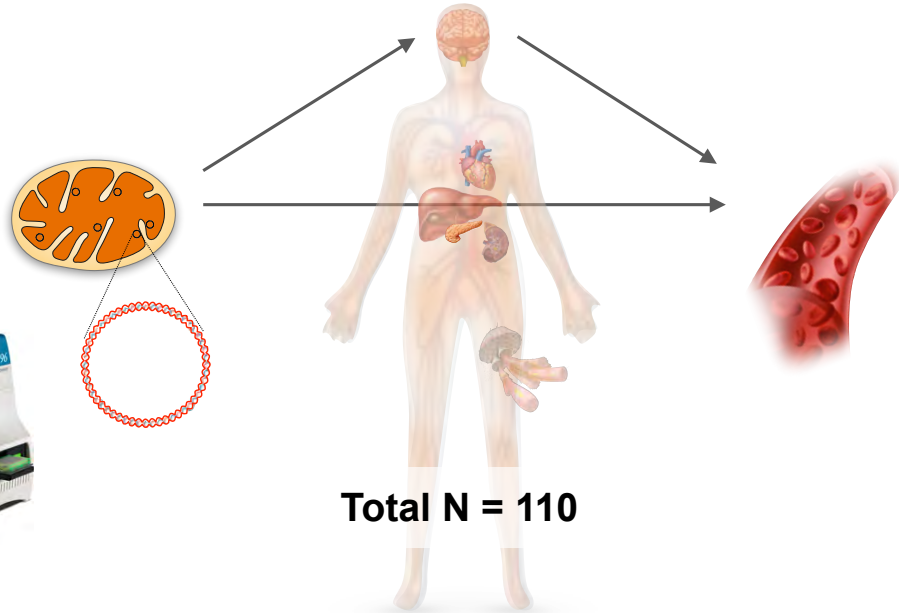
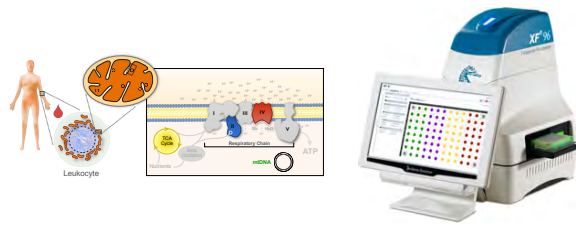


How much of inter-individual differences in **behaviors** are driven by **mitochondria**?

Mitochondrial Stress, Brain Imaging, and Epigenetics — MiSBIE

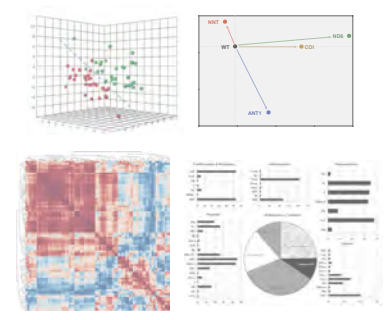


mtDNA heteroplasmy
Mitochondrial OxPhos
Lymphocytes, Monocytes,
Neutrophils, Platelets

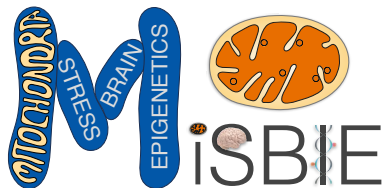


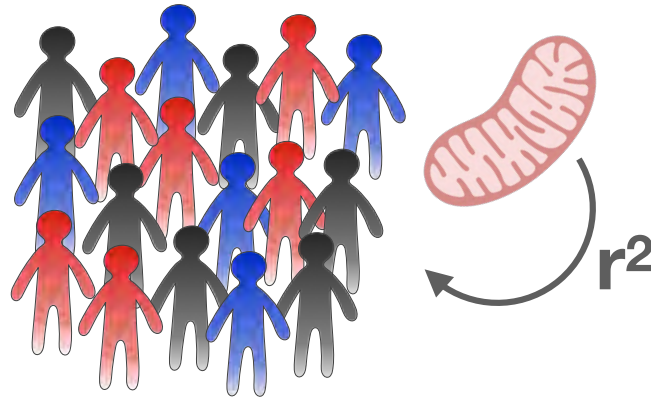
Total N = 110

Disease biomarkers
Stress reactivity
Energy expenditure
e.g., GDF15, Lactate,
Pyruvate, Alanine, etc.

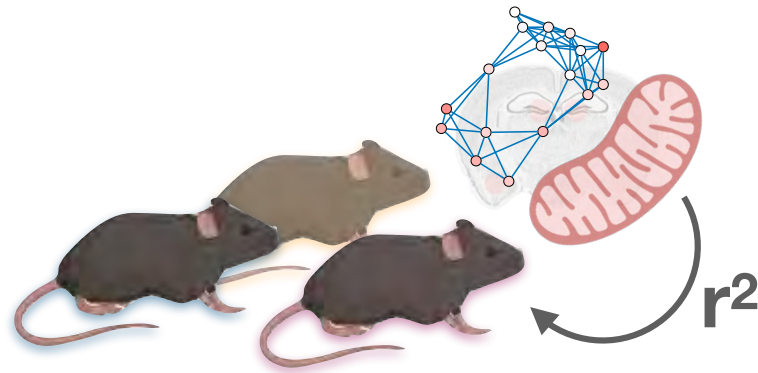


- **Healthy controls** (n = 70)
- **mtDNA defects**
 - 3243A>G (group A) (n = 20)
 - 3243A>G (group B) (n = 5)
 - Single deletion (n = 15)

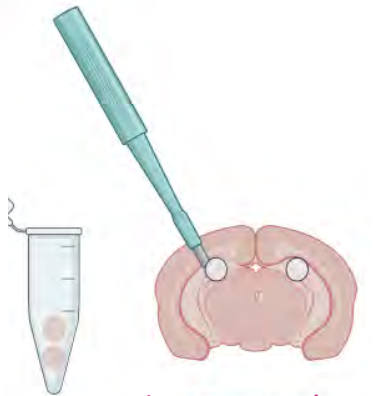
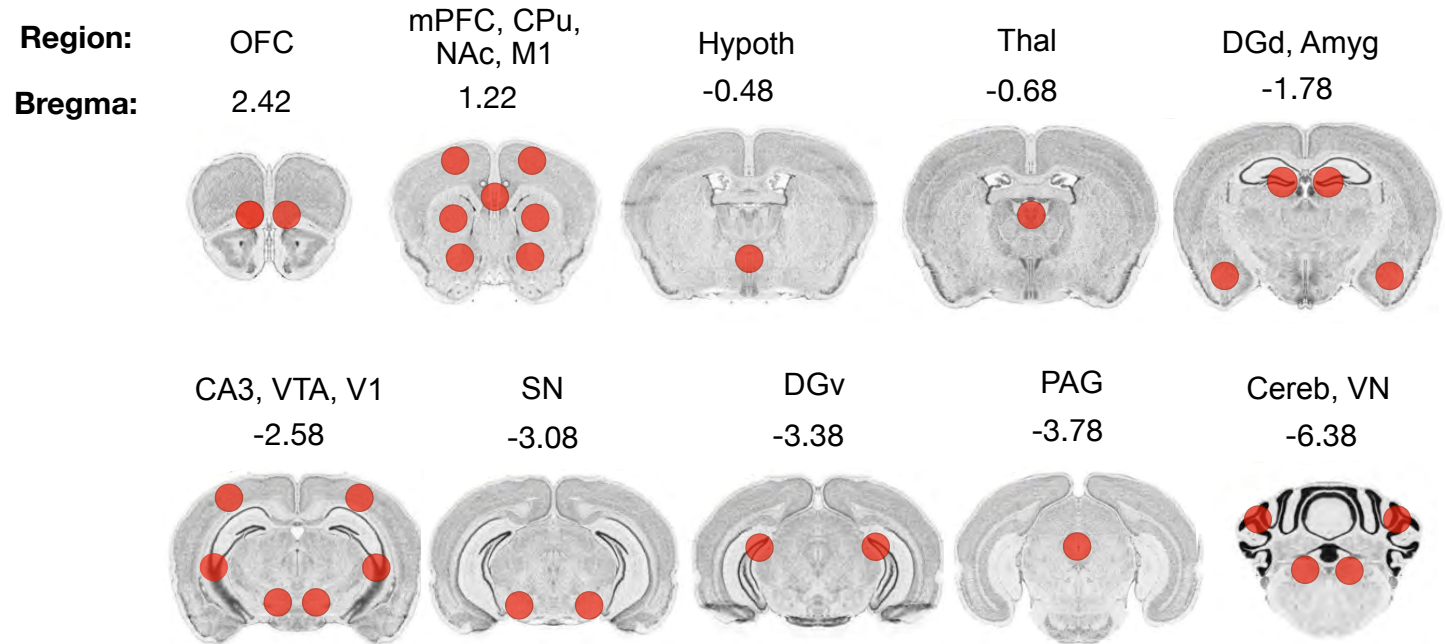




How much of inter-individual differences in **behaviors** are driven by **mitochondria**?



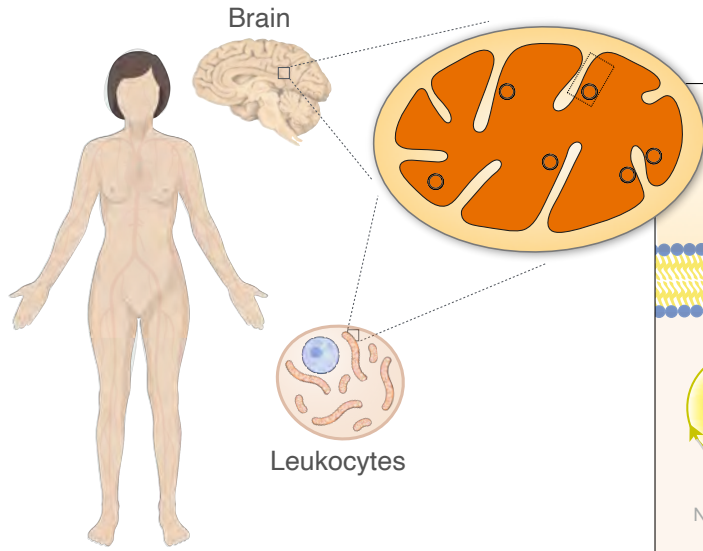
Mitochondrial functional profiling in the mouse brain



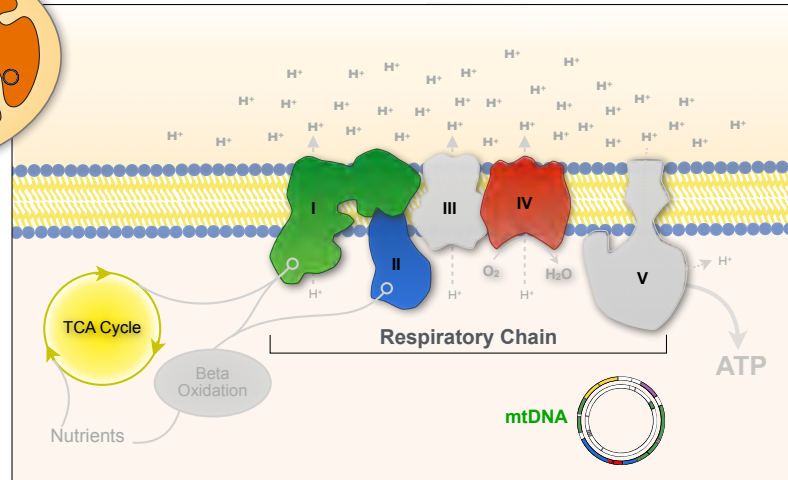
1mm punches
(n=17)

Each punch is <1mg
n > 500 samples

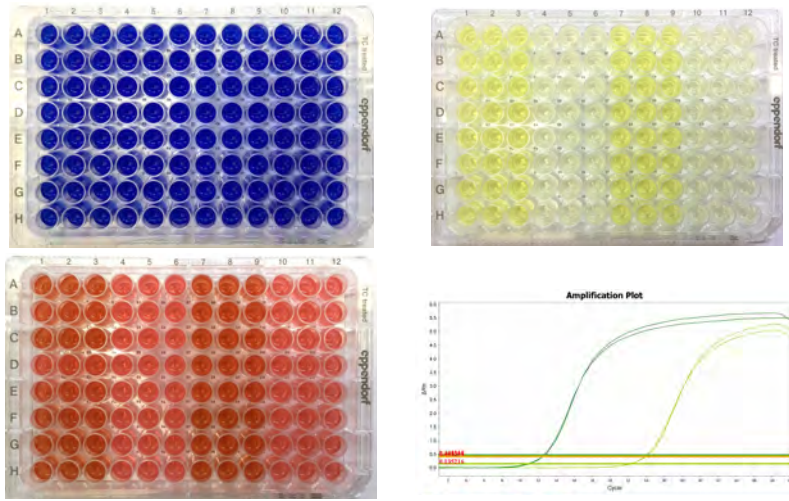




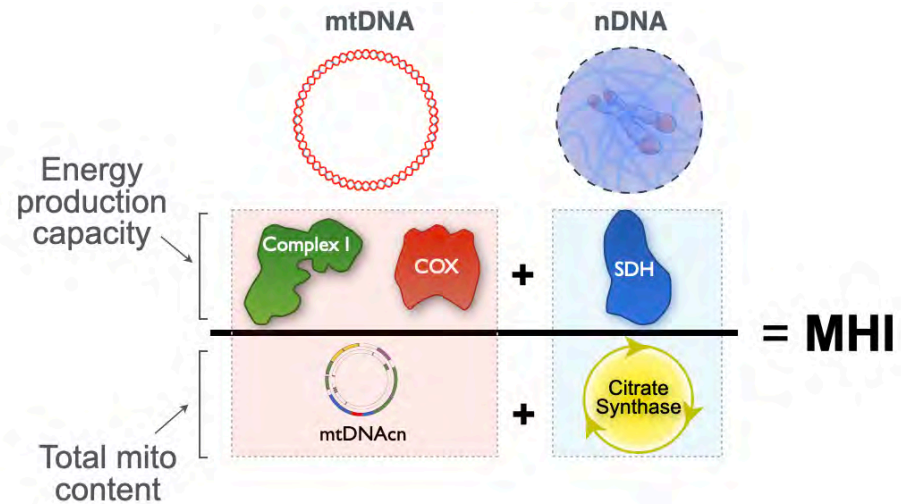
Enzymatic activity assays



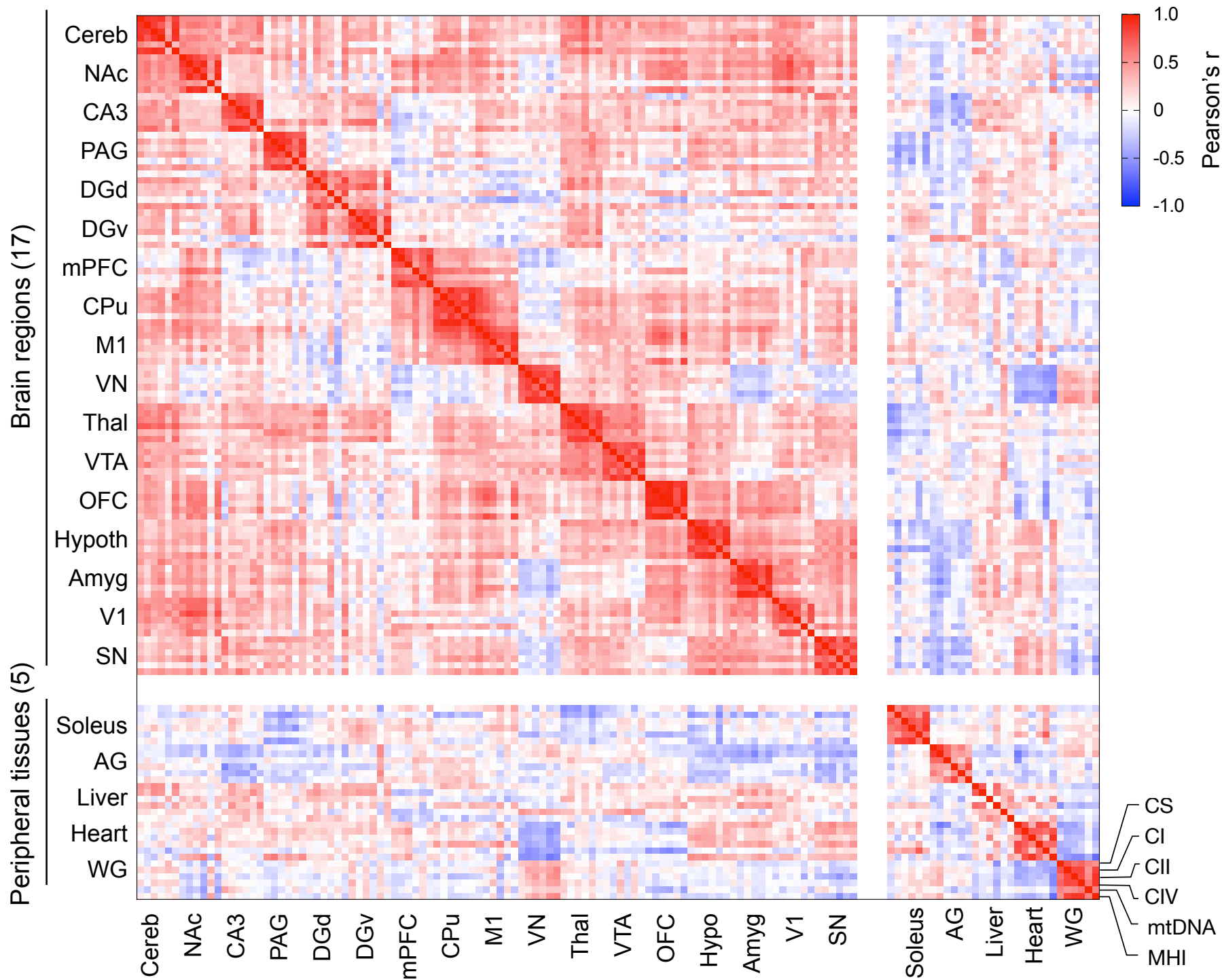
Miniaturization & optimized throughput



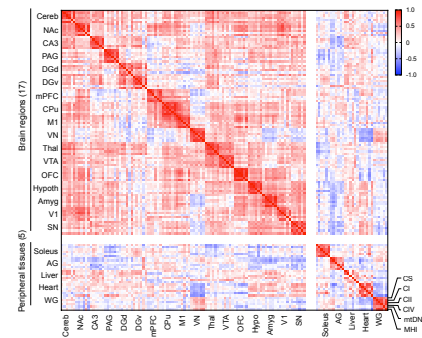
Computational integration



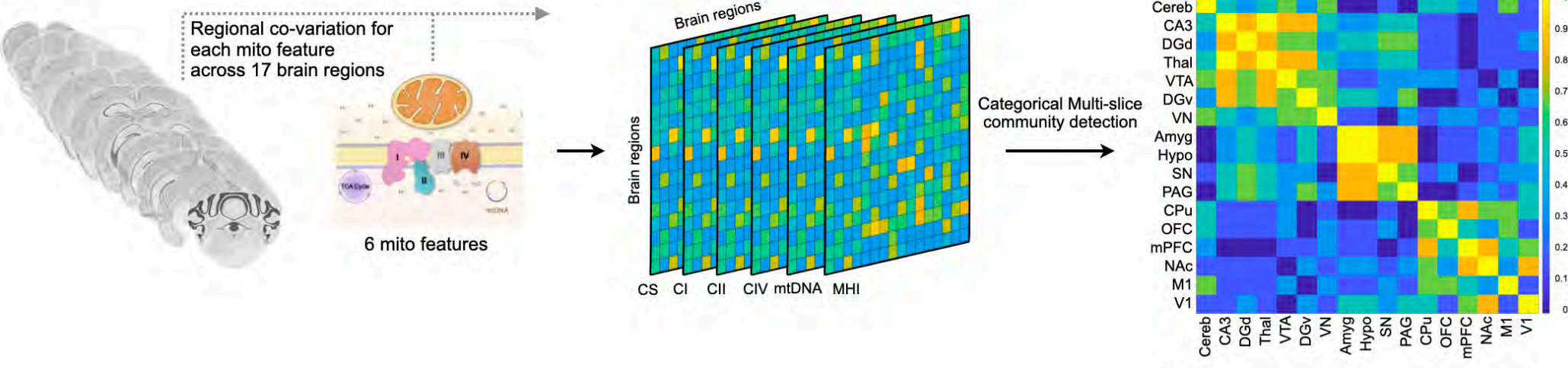
Similarity matrix based on mitochondrial activities



Are there brain networks with shared mitochondrial phenotypes?

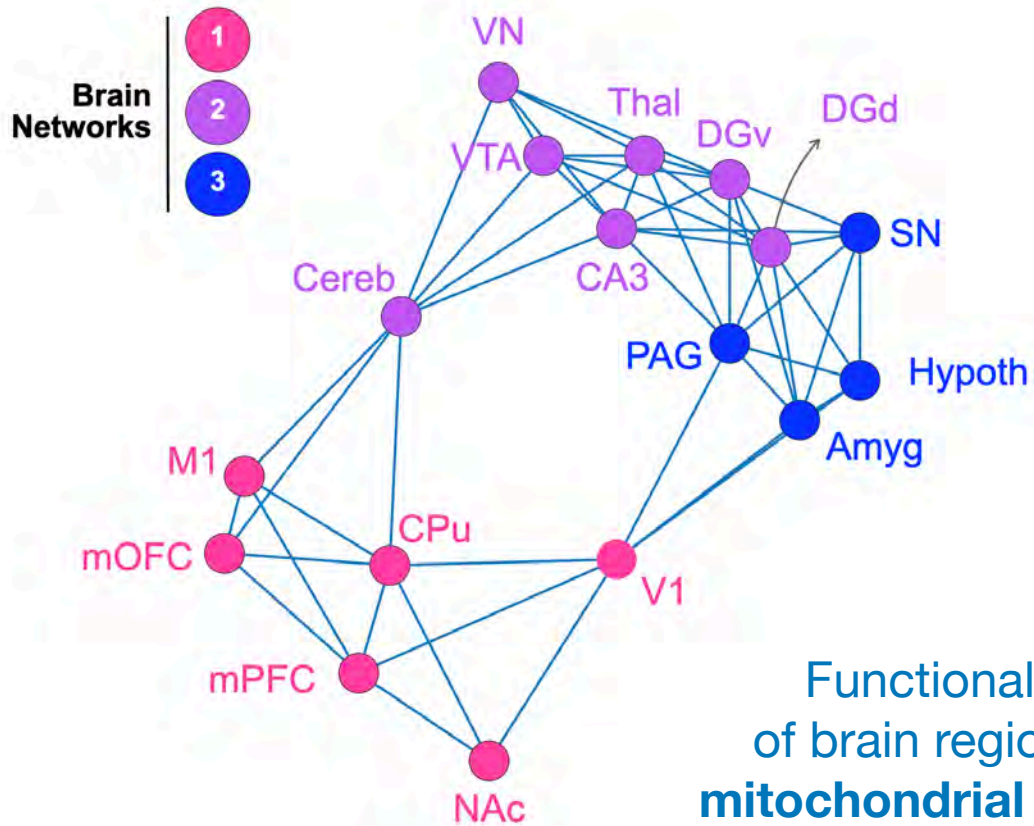
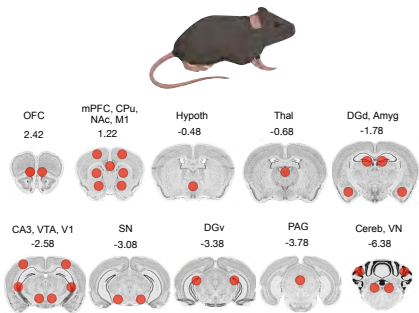
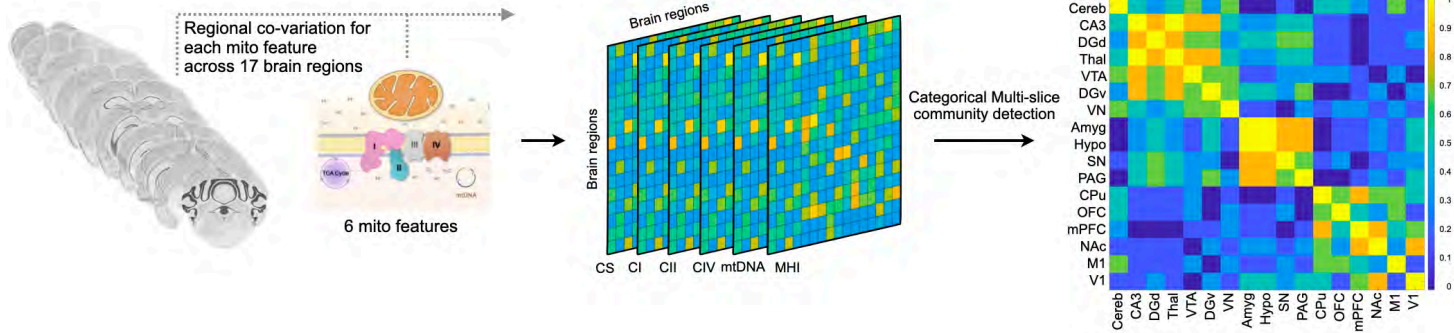


Mitochondria-driven community detection among brain regions



Manish Saggar

Mitochondria-driven community detection among brain regions



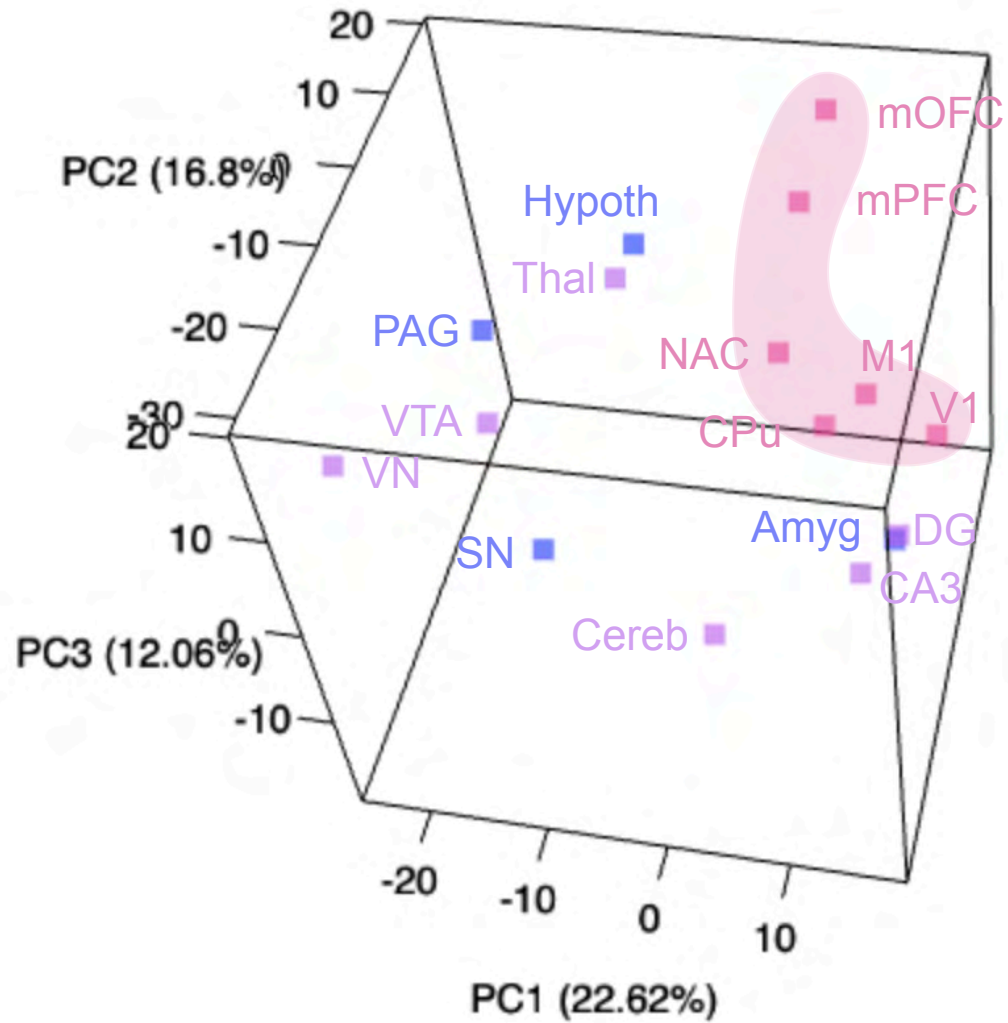
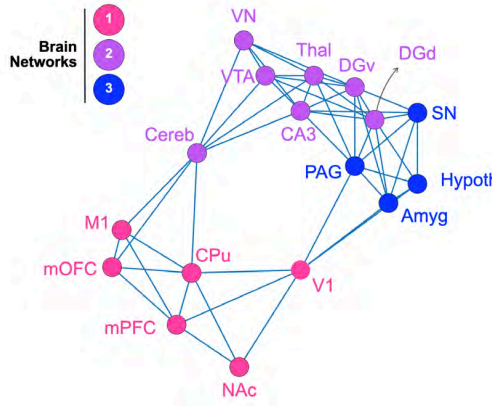
Functional clustering of brain regions based on mitochondrial “connectivity”



Manish Saggar

946 mitochondrial genes

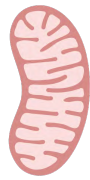
PCA: Shared mitochondrial gene signature



Jack Devine



Anna Monzel

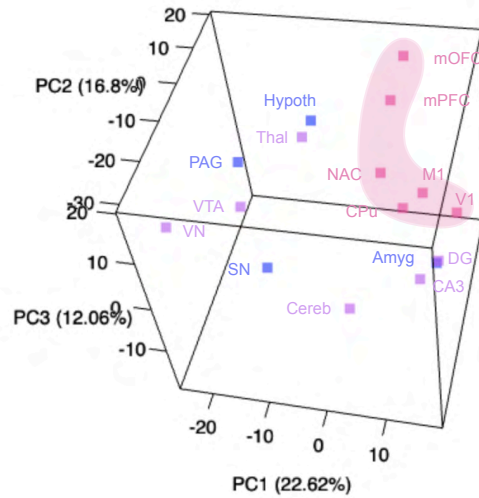


Enrichment of *mitochondrial* genes and pathways

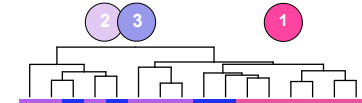
946 mitochondrial **genes**

149 mitochondrial **pathways**

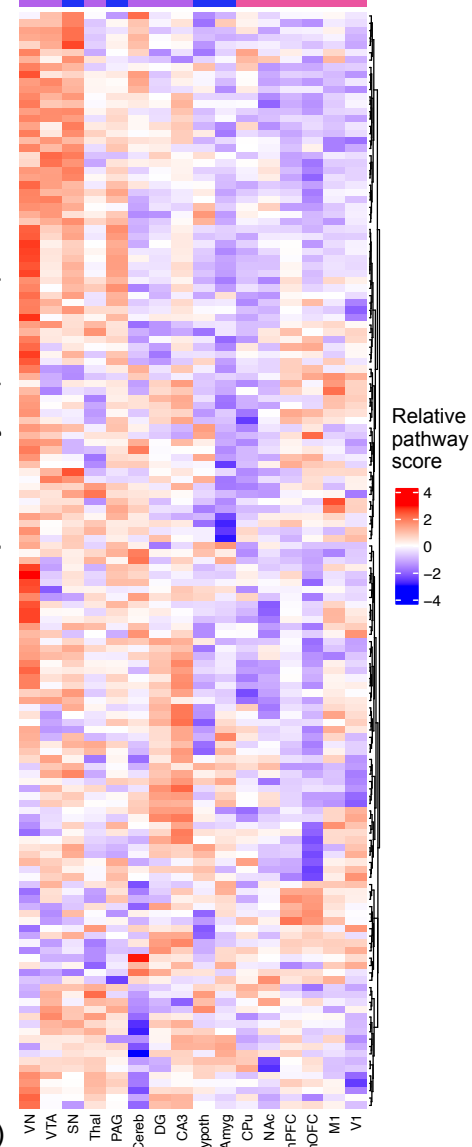
PCA: Shared mitochondrial **gene signature**



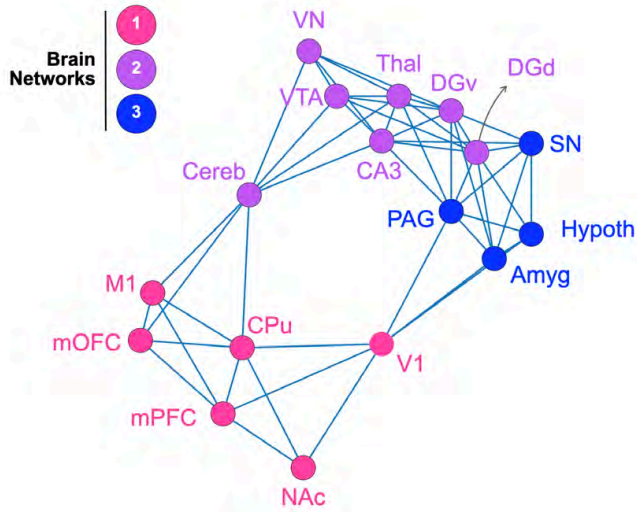
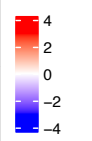
Hierarchical clustering: Shared mitochondrial **pathway signature**



Mitochondrial pathways (n=149)



Relative pathway score



Jack Devine

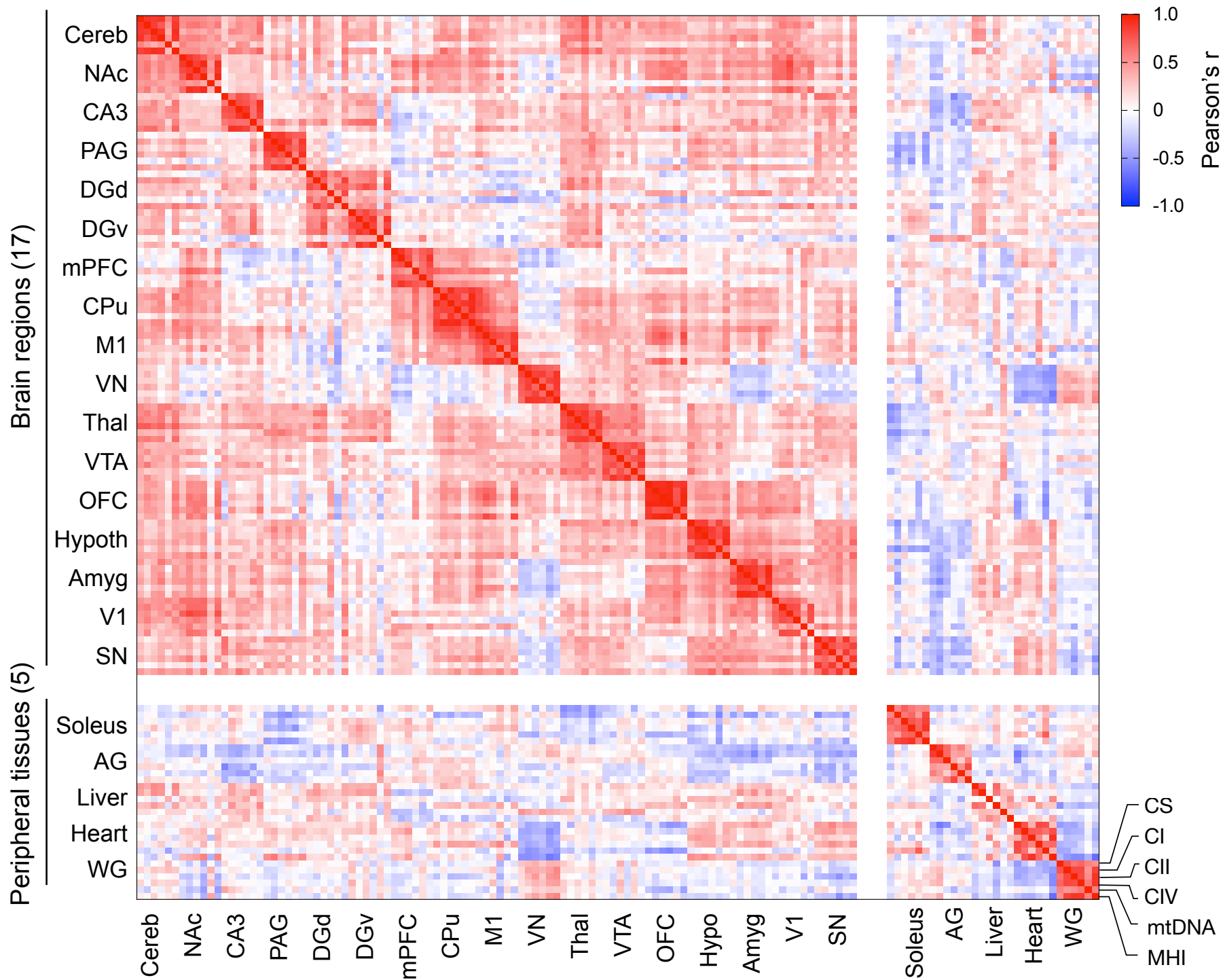


Anna Monzel

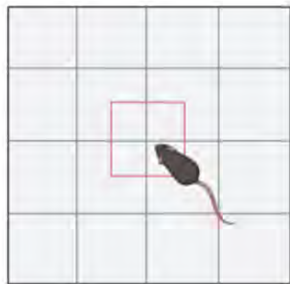
Data from *Allen Mouse Brain Atlas*
Mitopathways from *MitoCarta 3.0*

Brain areas (n=17)

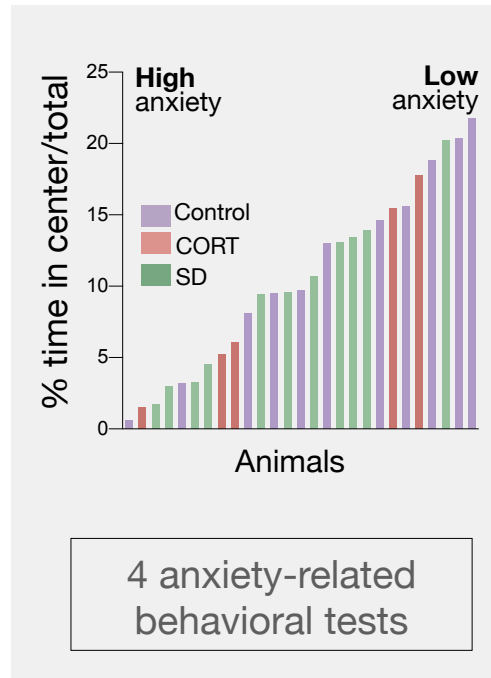
Similarity matrix based on mitochondrial activities



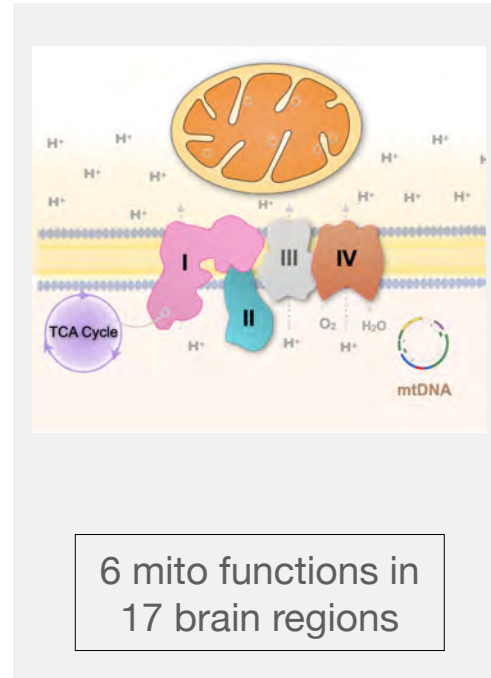
Mitochondria-behavior correlations



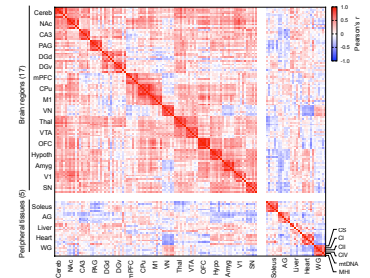
Open Field Test



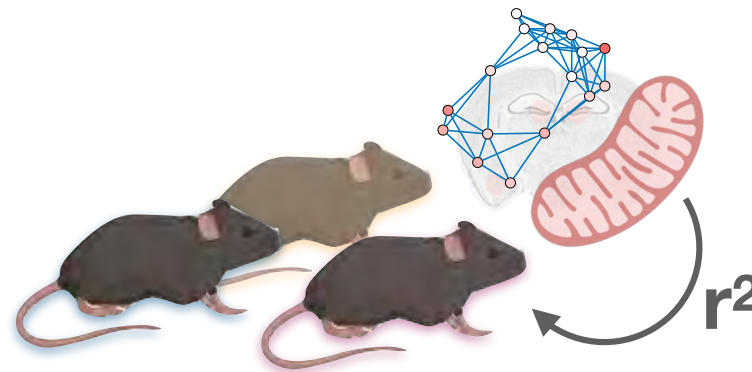
4 anxiety-related behavioral tests

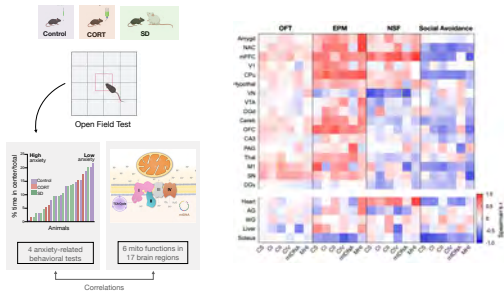


6 mito functions in 17 brain regions

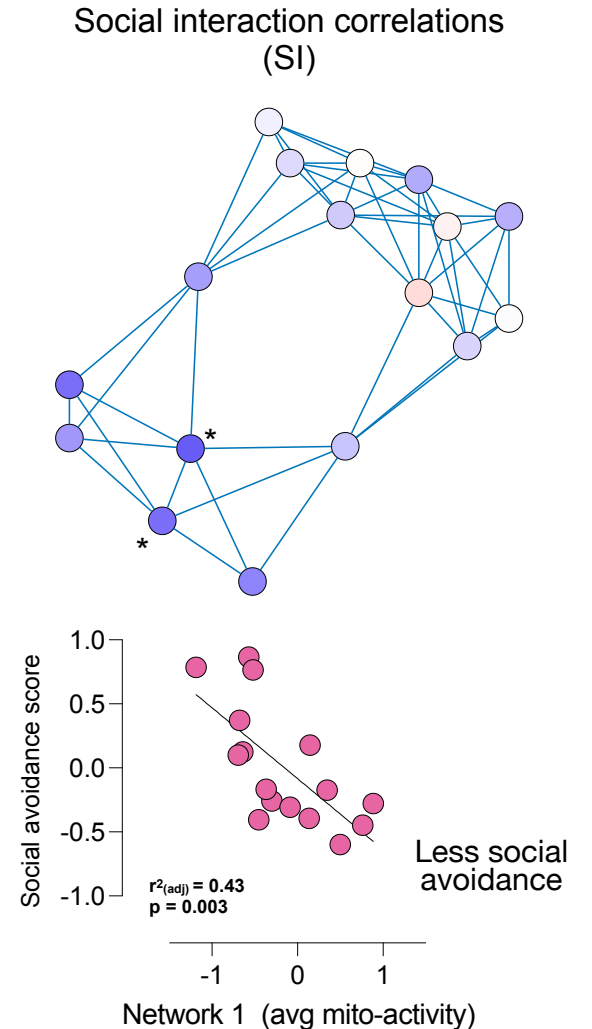
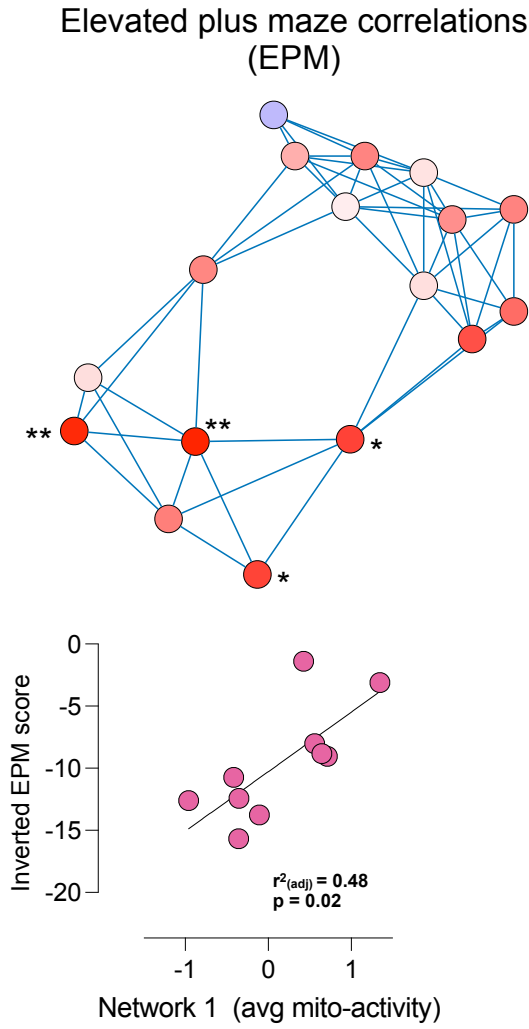
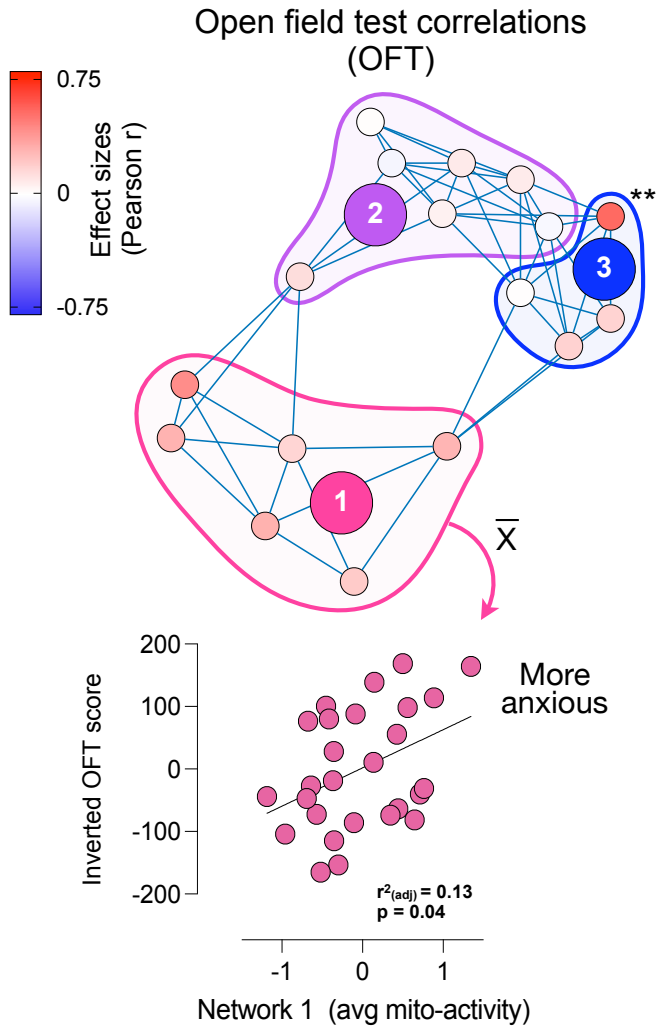
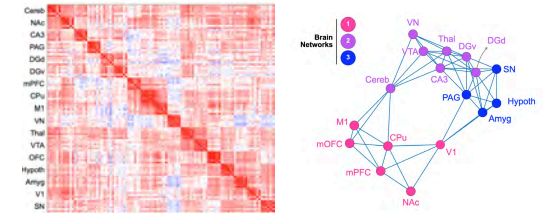


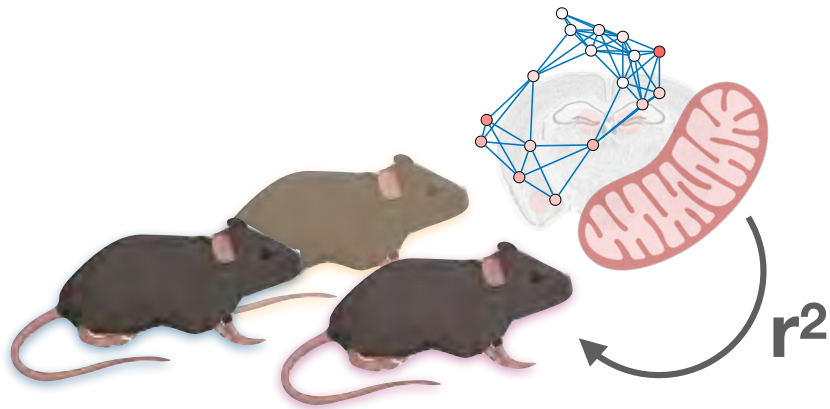
Correlations



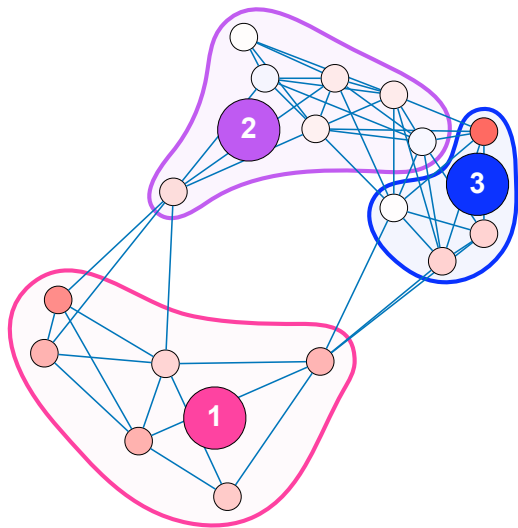


Network-based mito-behavior correlations

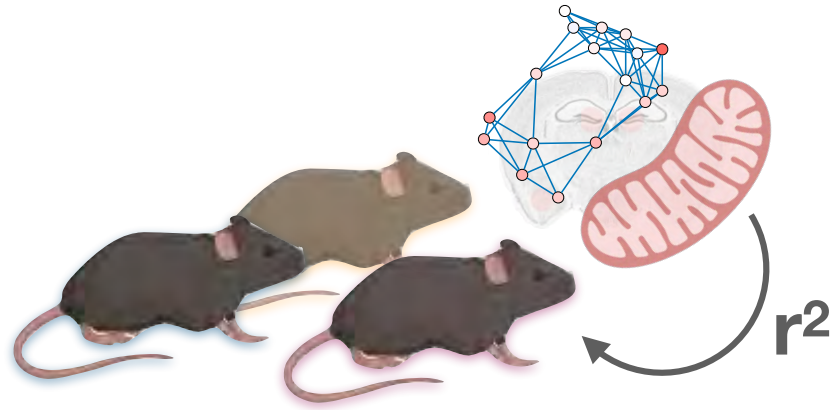




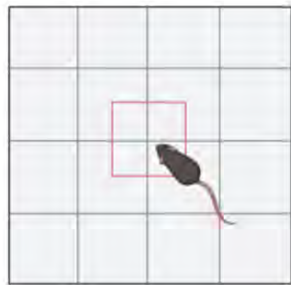
Network-based mito-behavior correlations



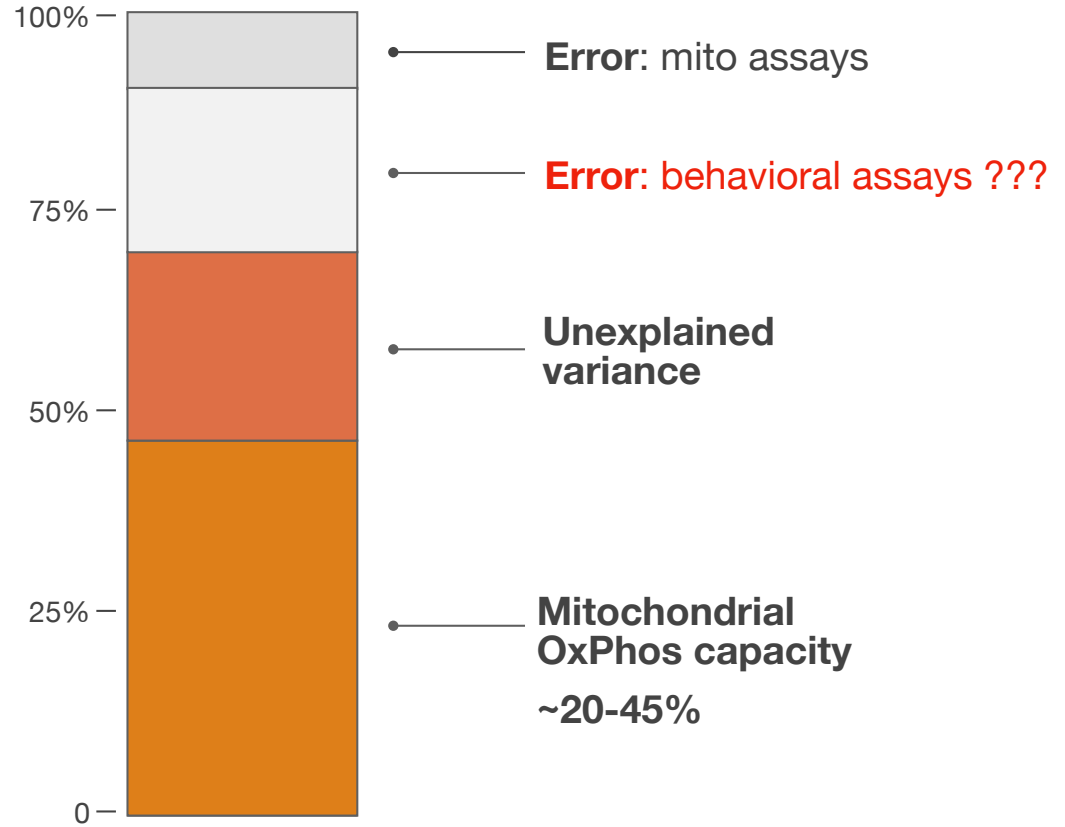
Brain mitochondria account for **up to ~20-45%** of the explainable variance in behaviors between animals



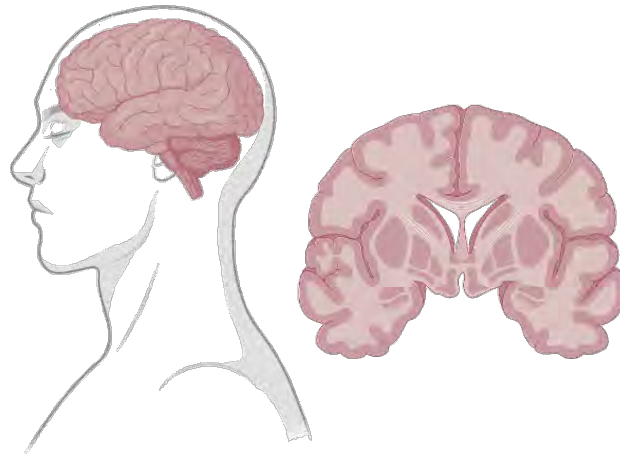
**TOTAL OBSERVED VARIANCE
IN ANIMAL BEHAVIORS**



Open Field Test

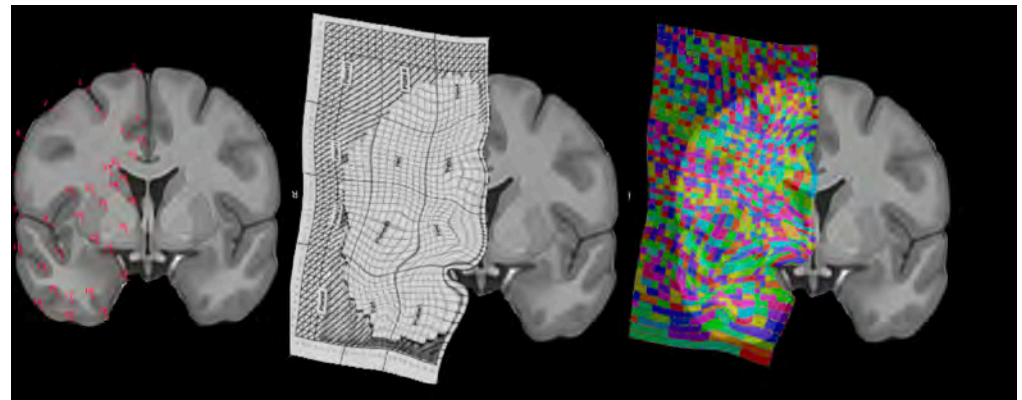
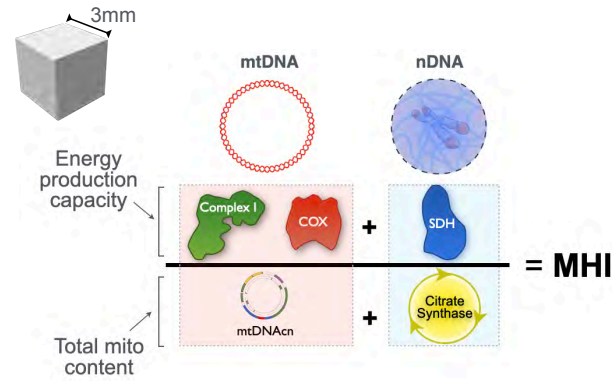
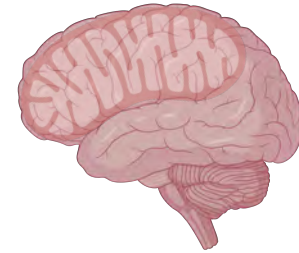


How are mitochondria distributed, and do they specialize across the *human* brain?



MitoBrainMap v1.0

A multi-function mitochondrial atlas of a single human coronal brain section at fMRI resolution

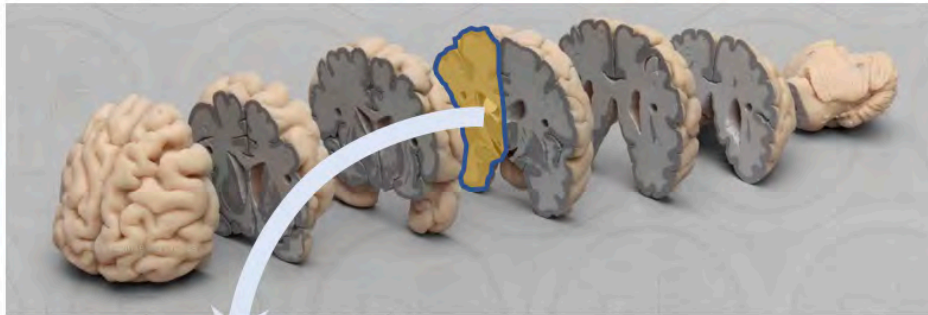


Closing the gap between organellar bioenergetic profiling and whole-brain neuroimaging modalities (fMRI, PET, CBV, DWI, etc)

Eugene Mosharov



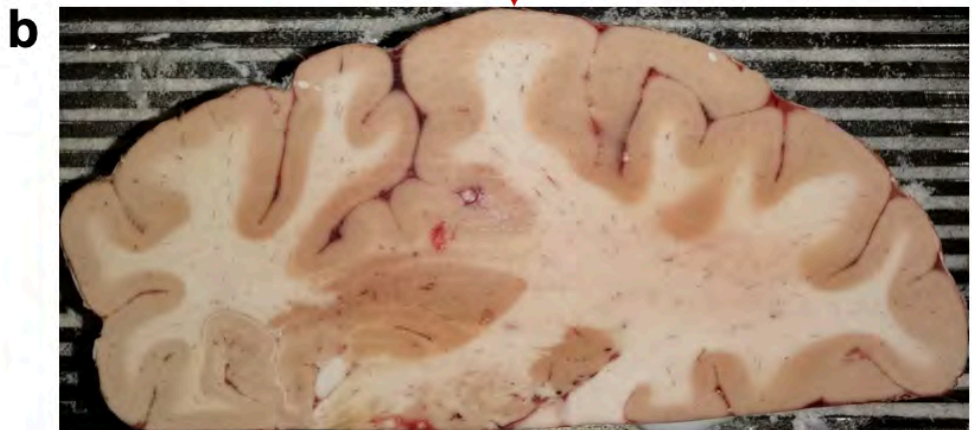
a Right hemisphere slab at MNI -15.51



Anterior surface of the frozen brain slab

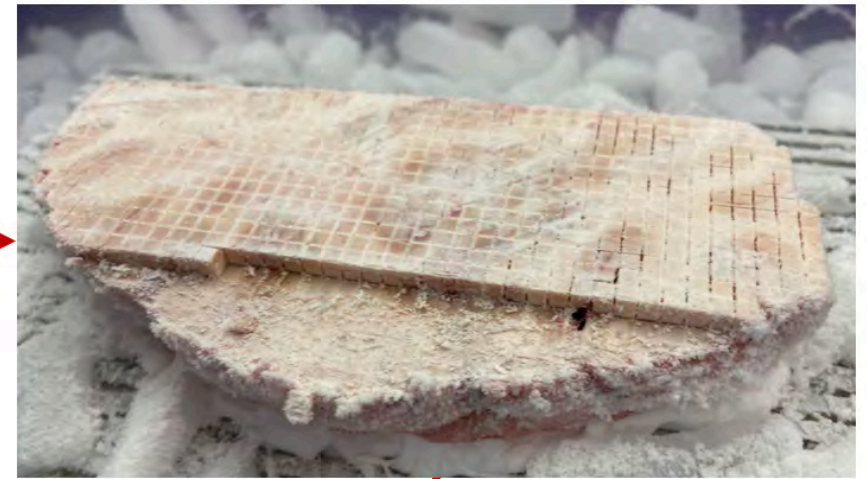


Cleaning (-1 mm)



Millina

d Collection



e Collection (-3 mm)

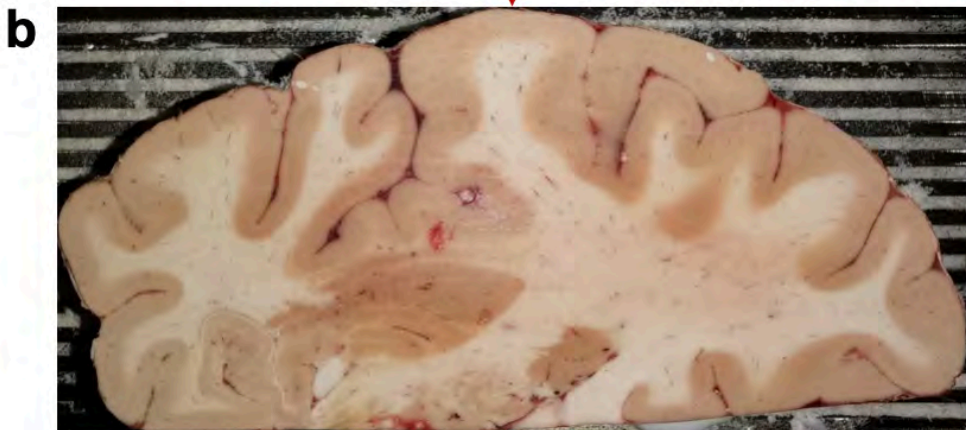


f Cleaning (-0.3 mm)

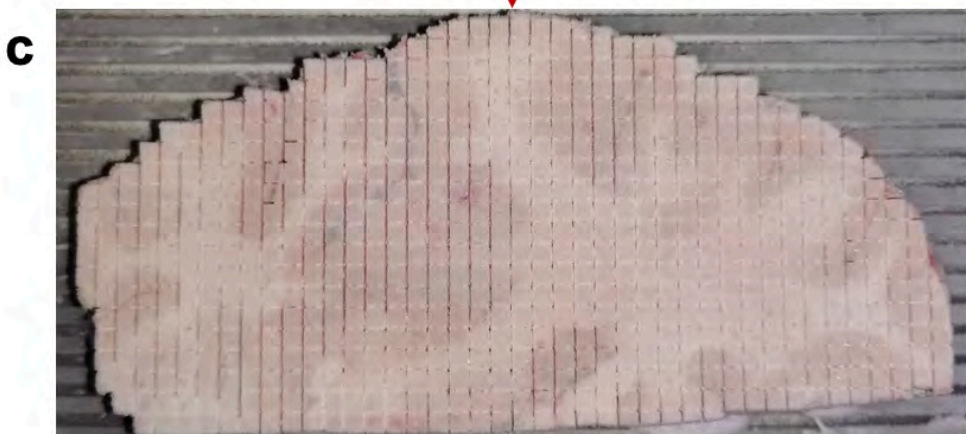




Cleaning (-1 mm)



Milling



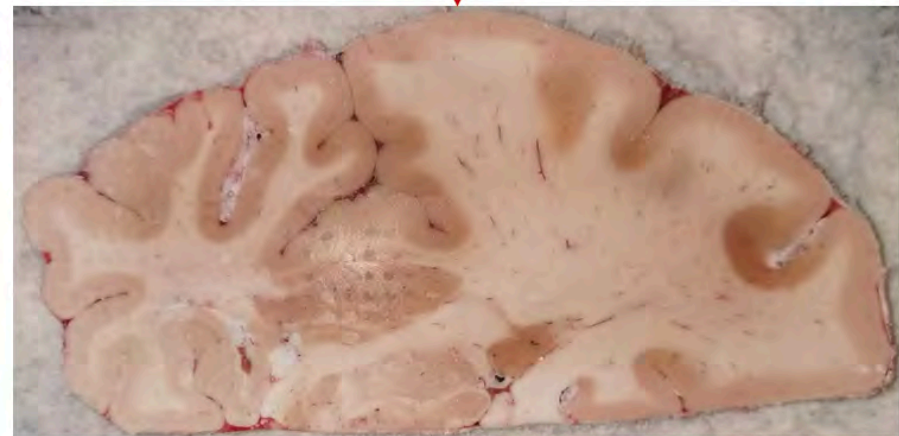
e

Collection (-3 mm)

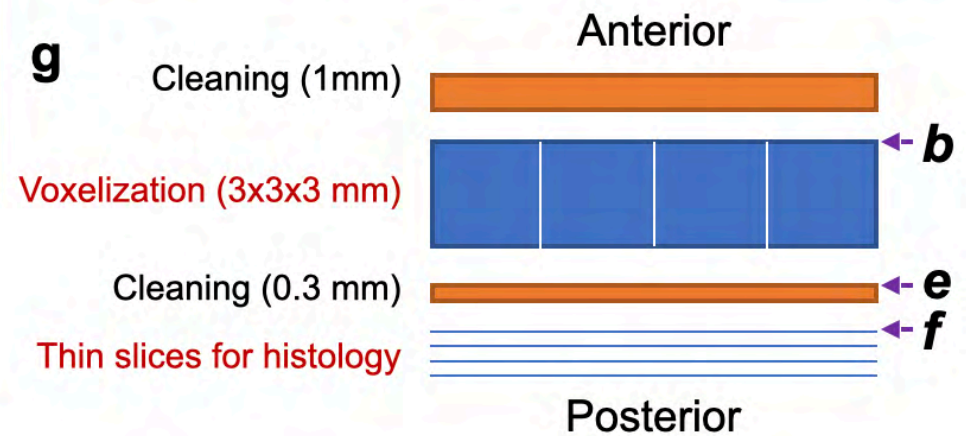


f

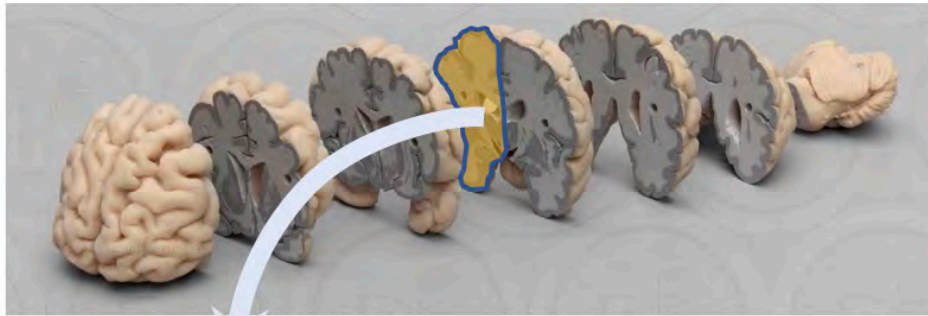
Cleaning (-0.3 mm)



g



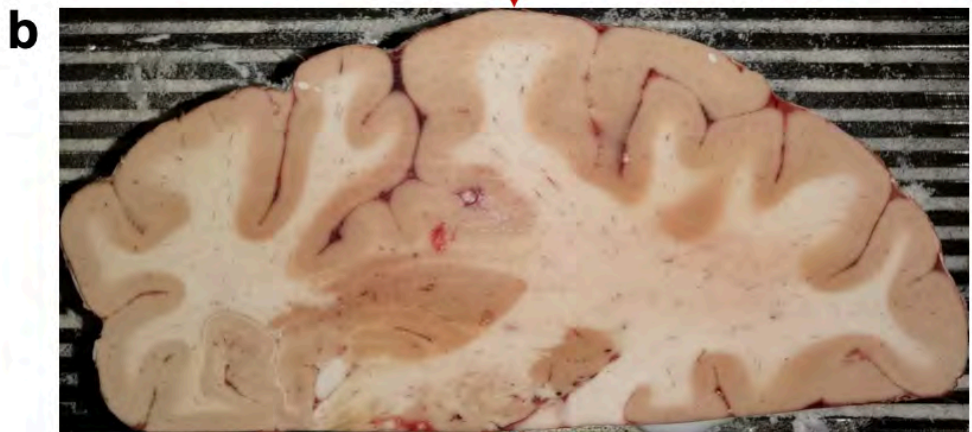
a Right hemisphere slab at MNI -15.51



Anterior surface of the frozen brain slab

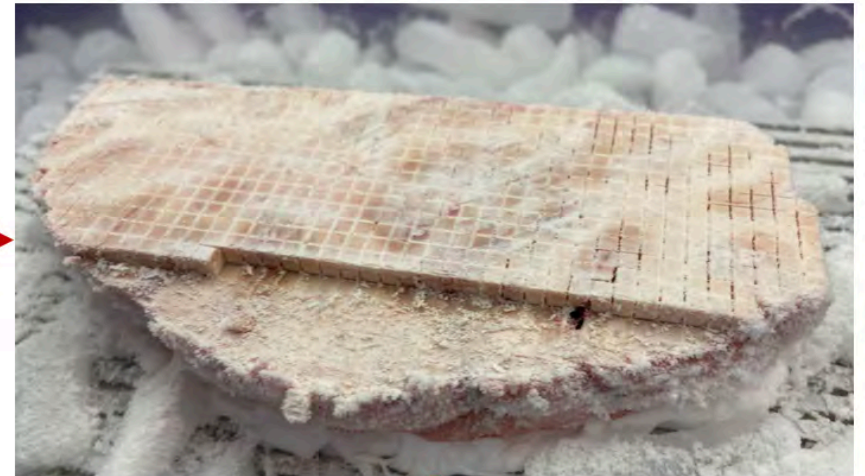


Cleaning (-1 mm)



Milling

d Collection



e Collection (-3 mm)



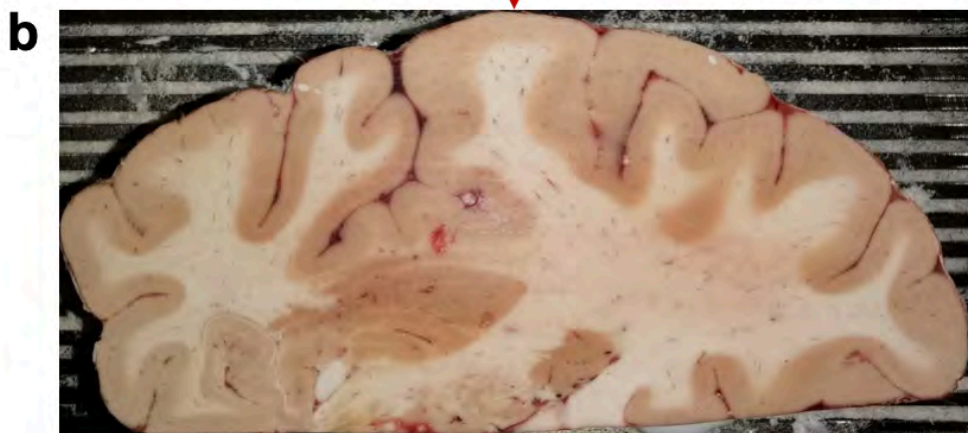
f Cleaning (-0.3 mm)



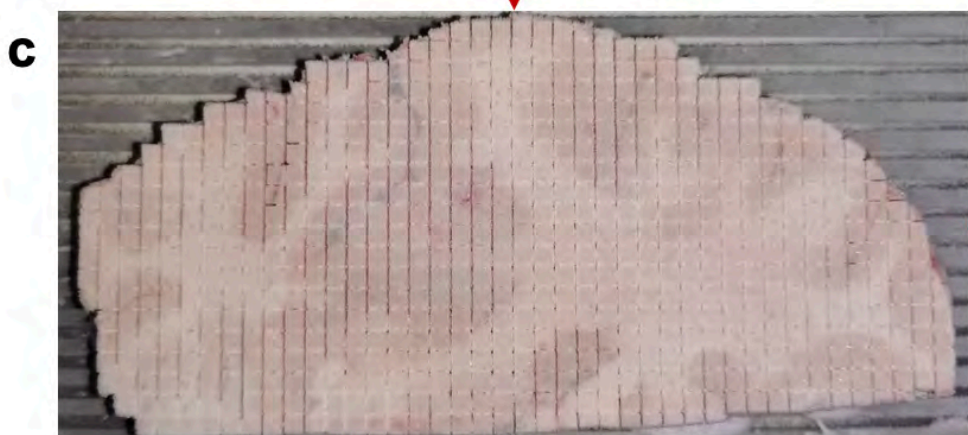
Anterior surface of the frozen brain slab



Cleaning (-1 mm)



Milling



e

Collection (-3 mm)



f

Cleaning (-0.3 mm)



g

Cleaning (1mm)

Anterior



Voxelization (3x3x3 mm)



Cleaning (0.3 mm)



Thin slices for histology



Posterior

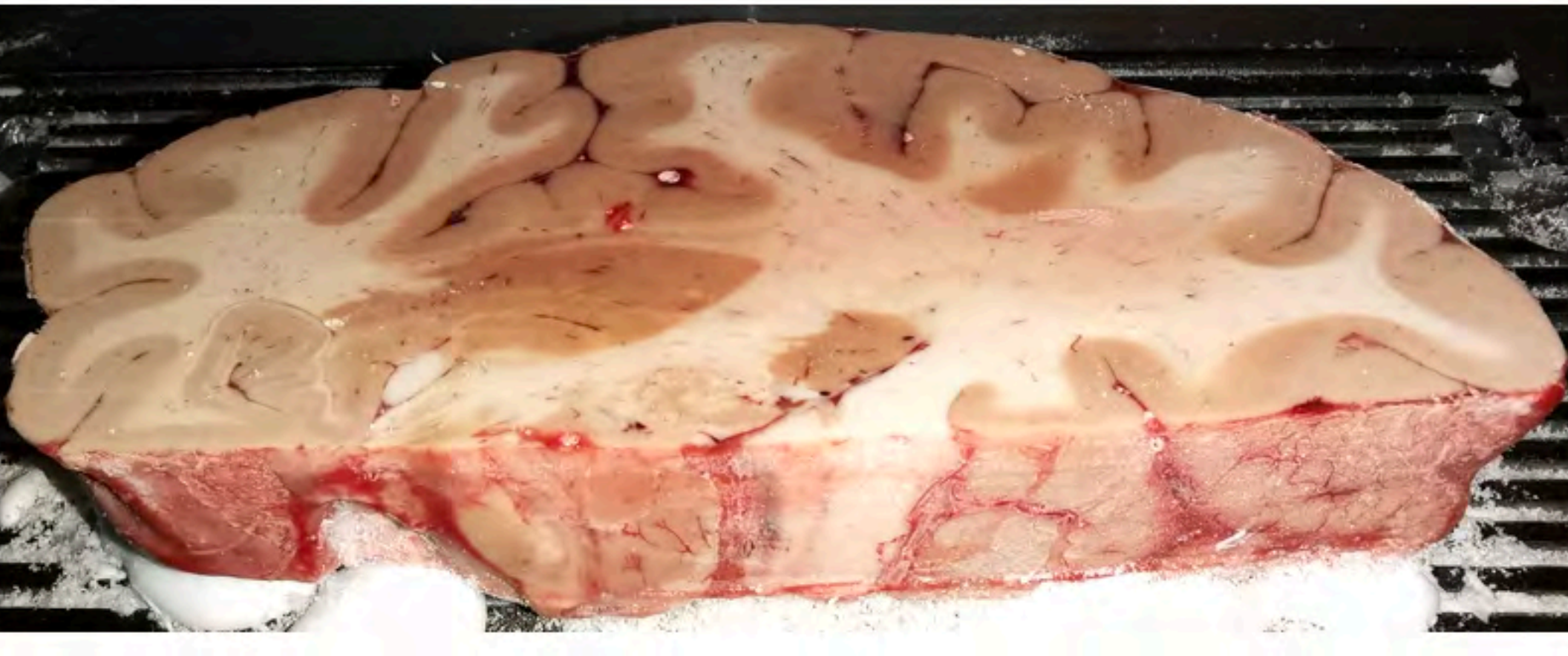
b

e

f

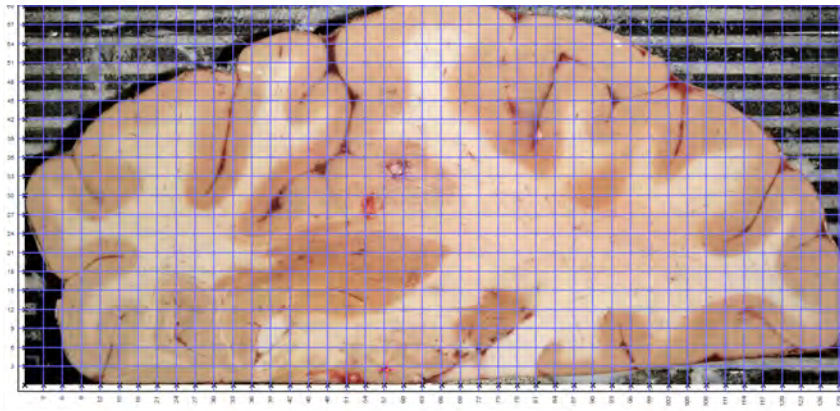
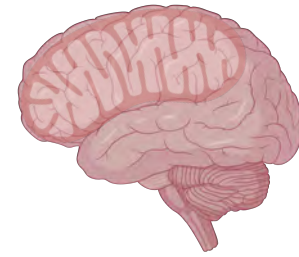
MitoBrainMap v1.0

A multi-function mitochondrial atlas of a single human coronal brain section at fMRI resolution

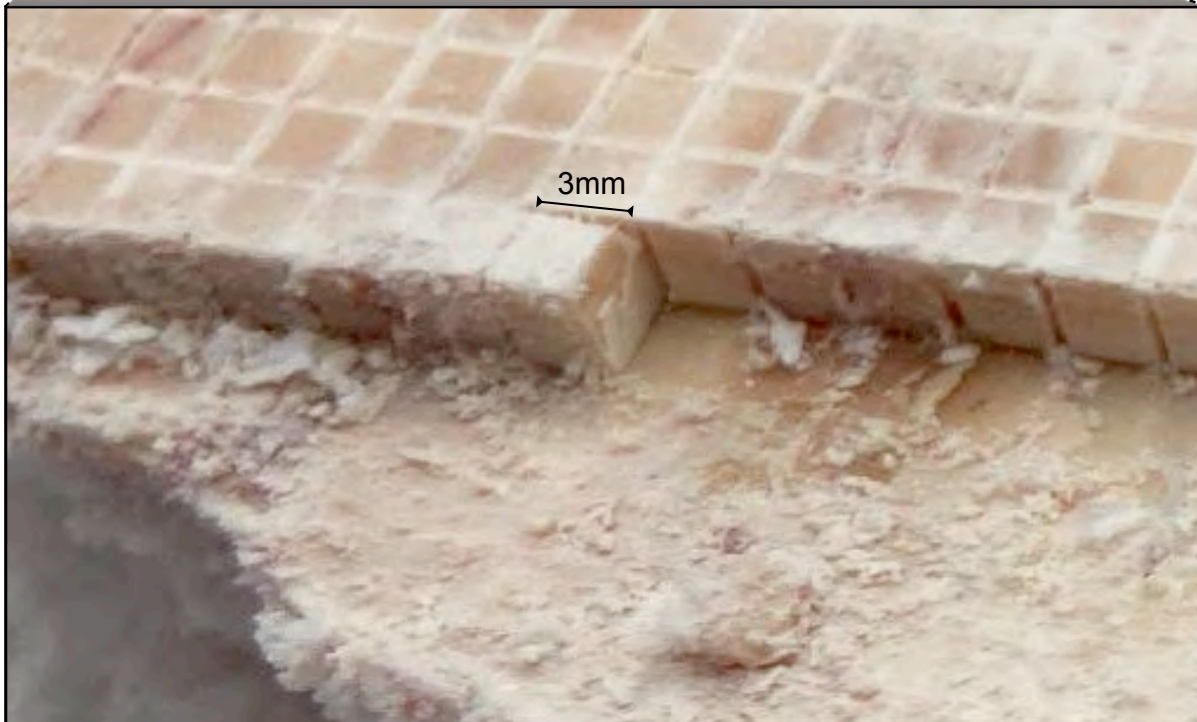
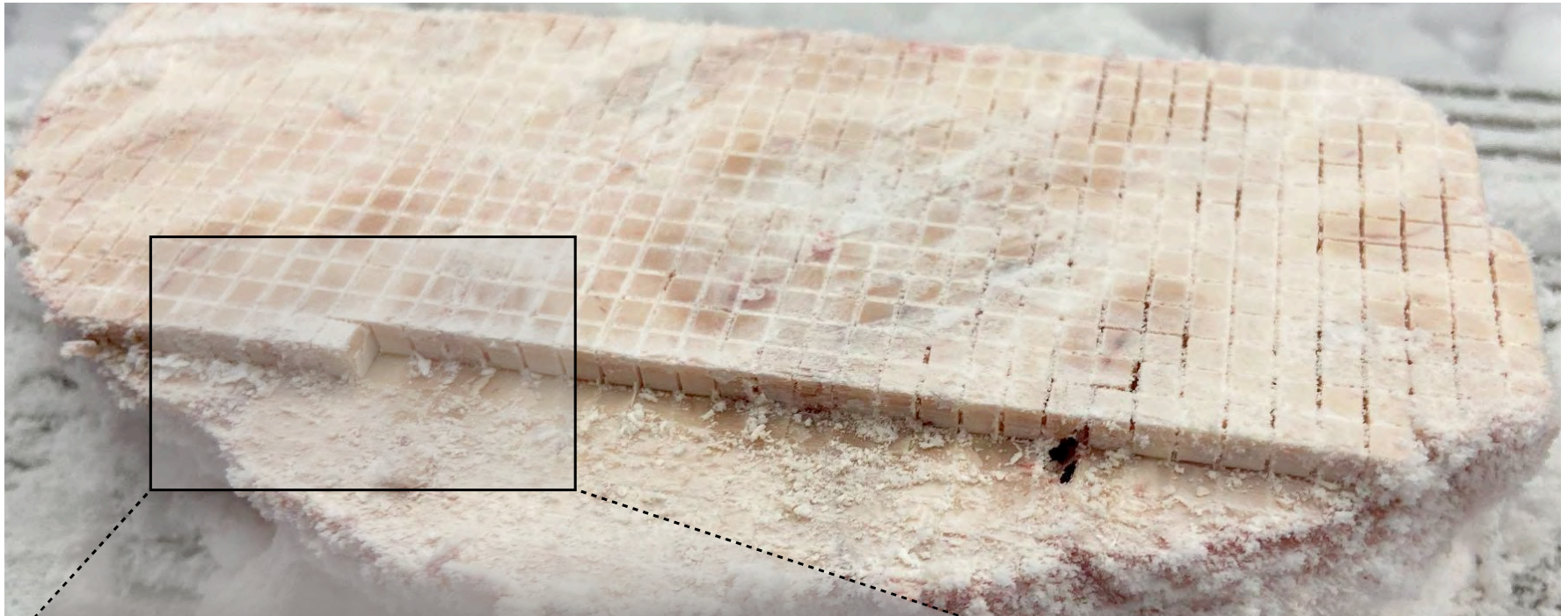


MitoBrainMap v1.0

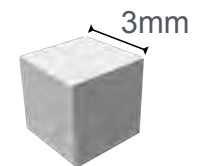
A multi-function mitochondrial atlas of a single human coronal brain section at fMRI resolution



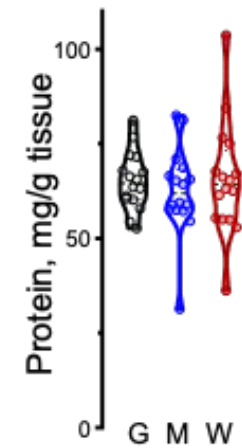
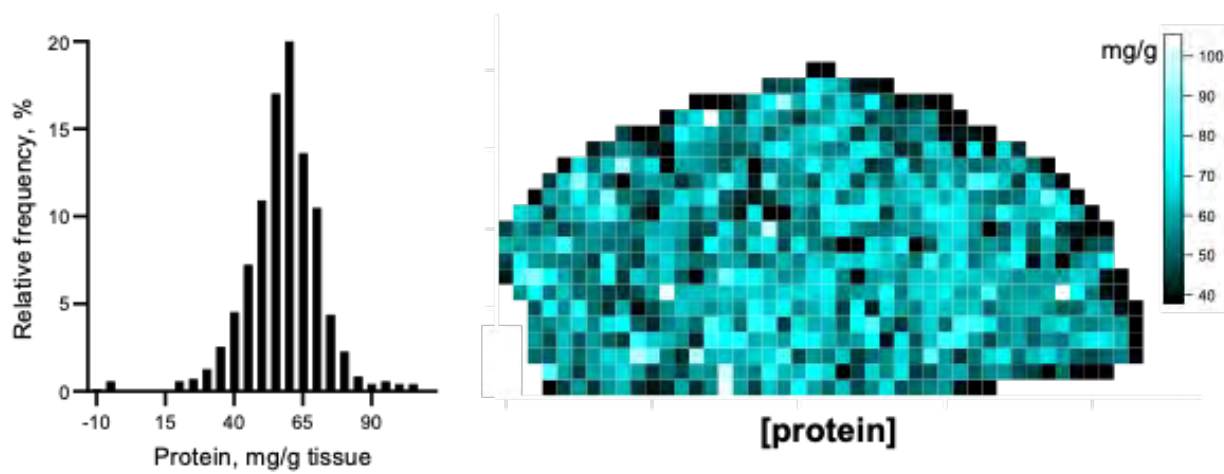
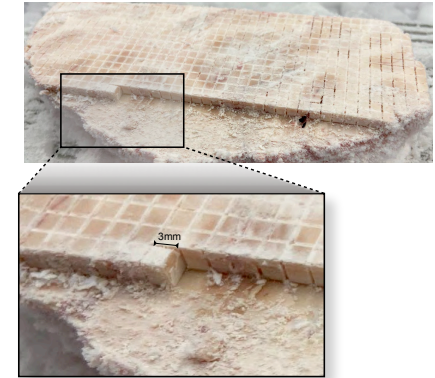
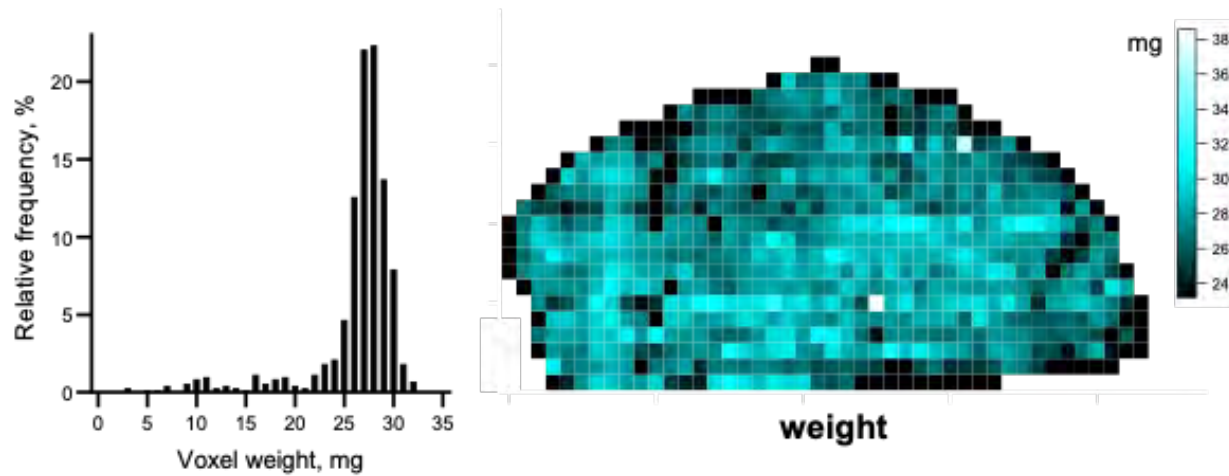
Eugene Mosharov

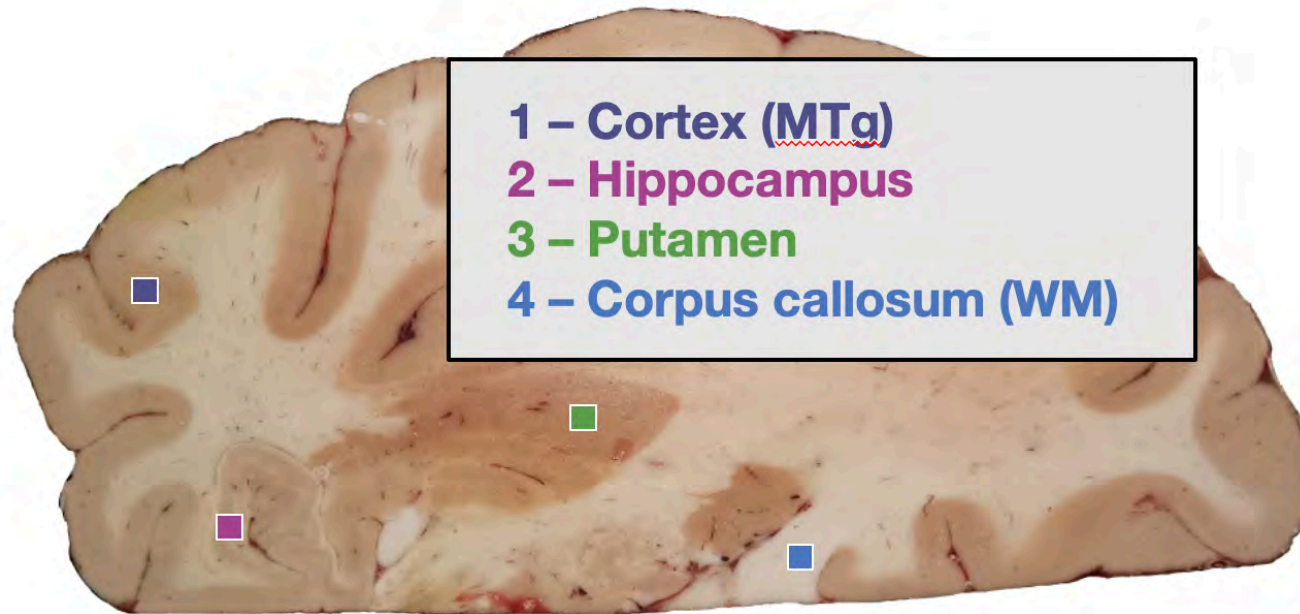


Physical *voxelization*
of the human brain
at fMRI resolution



Quality control on 702 human brain voxels



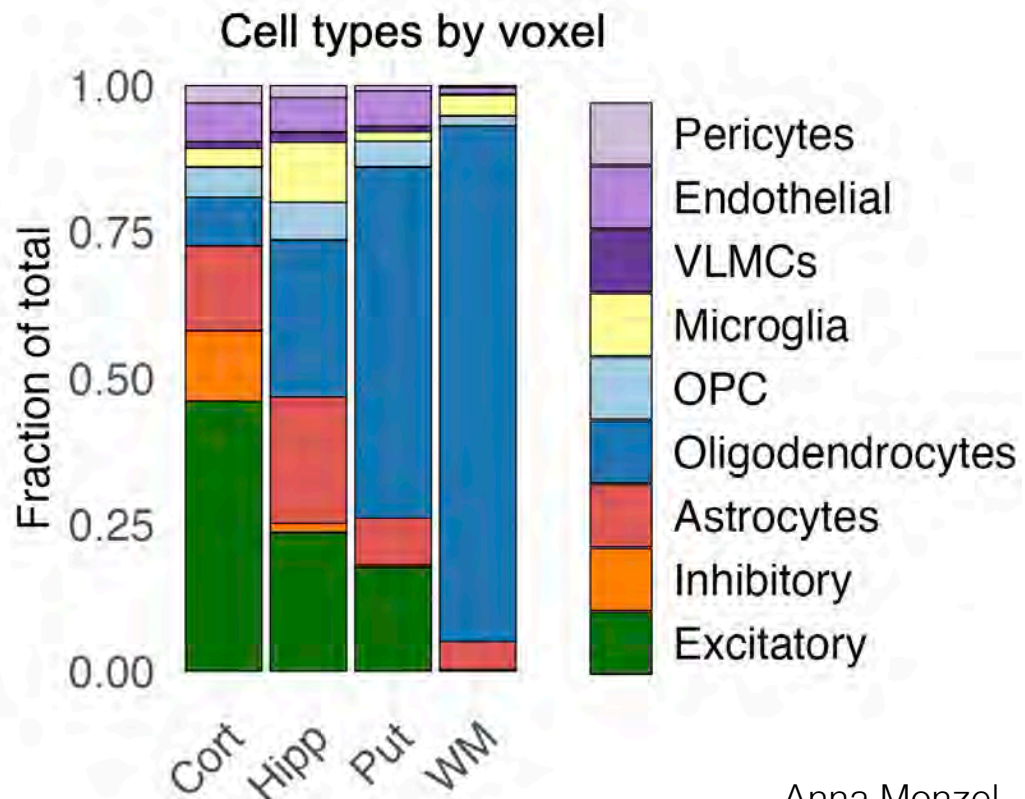
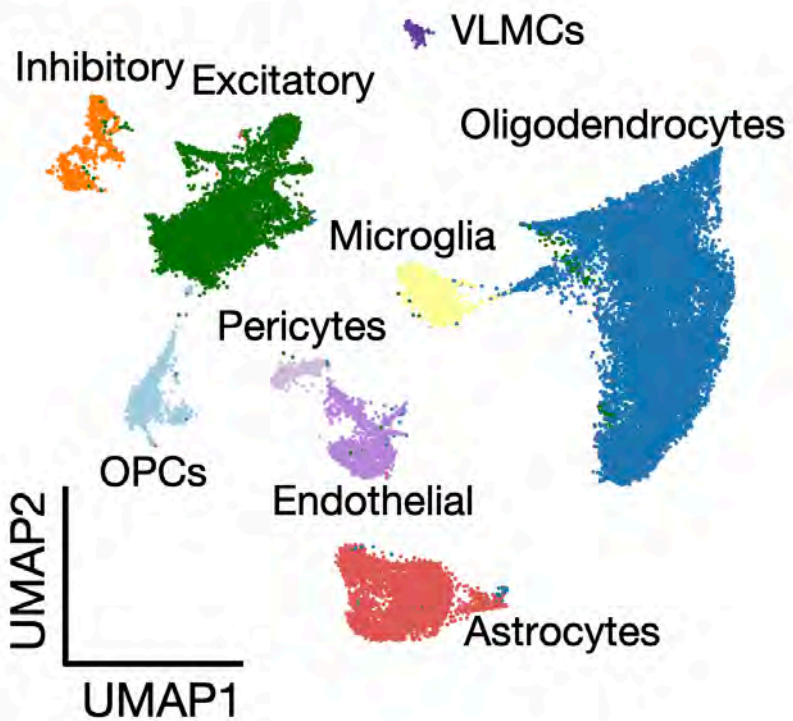
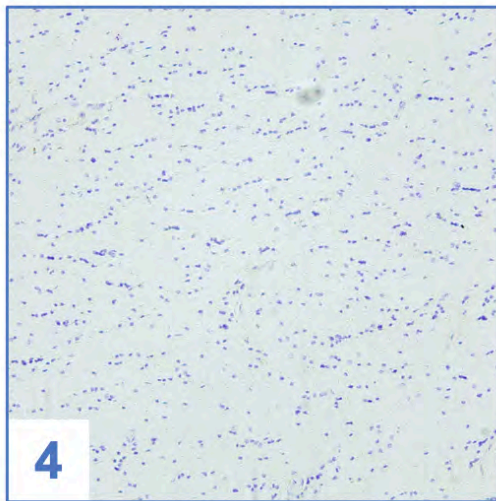
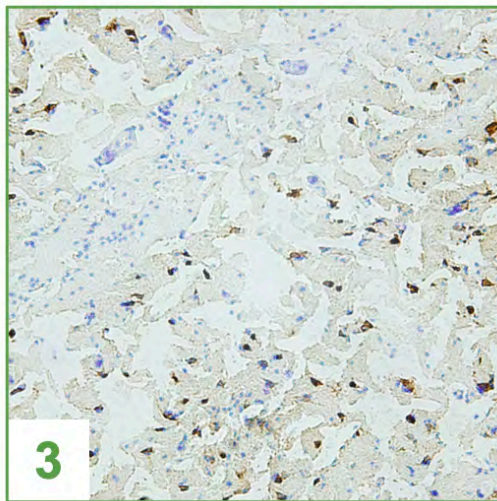
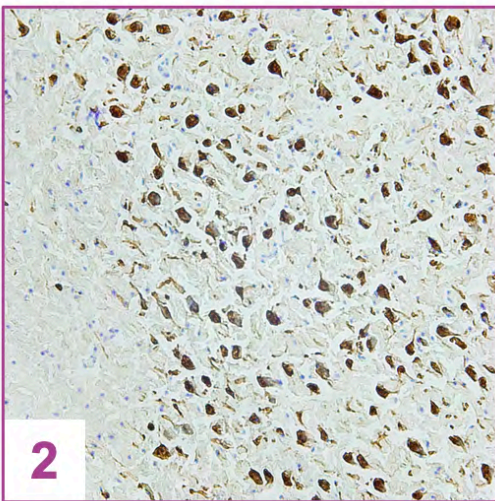
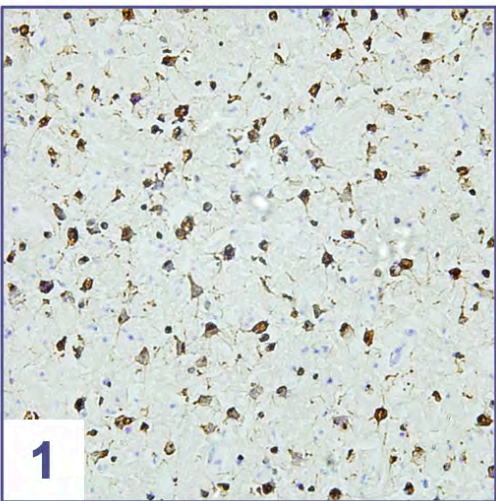
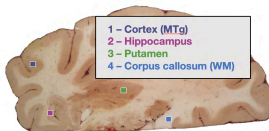


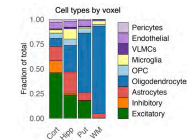
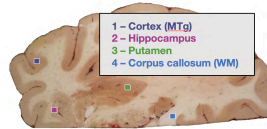
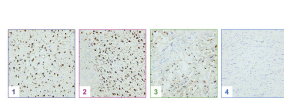
1 - Cortex (MTg)

2 - Hippocampus

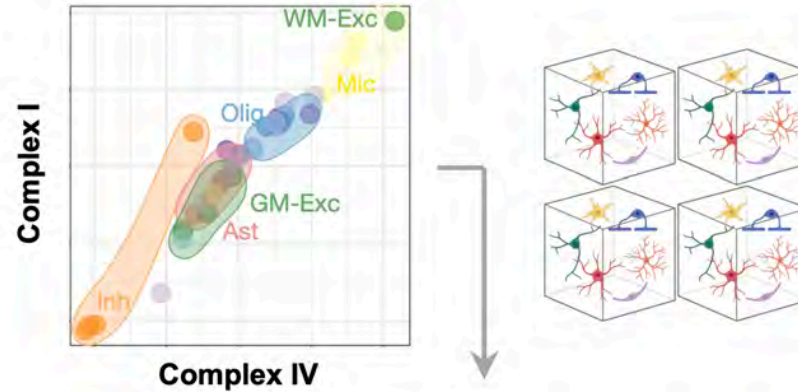
3 - Putamen

4 - Corpus callosum (WM)

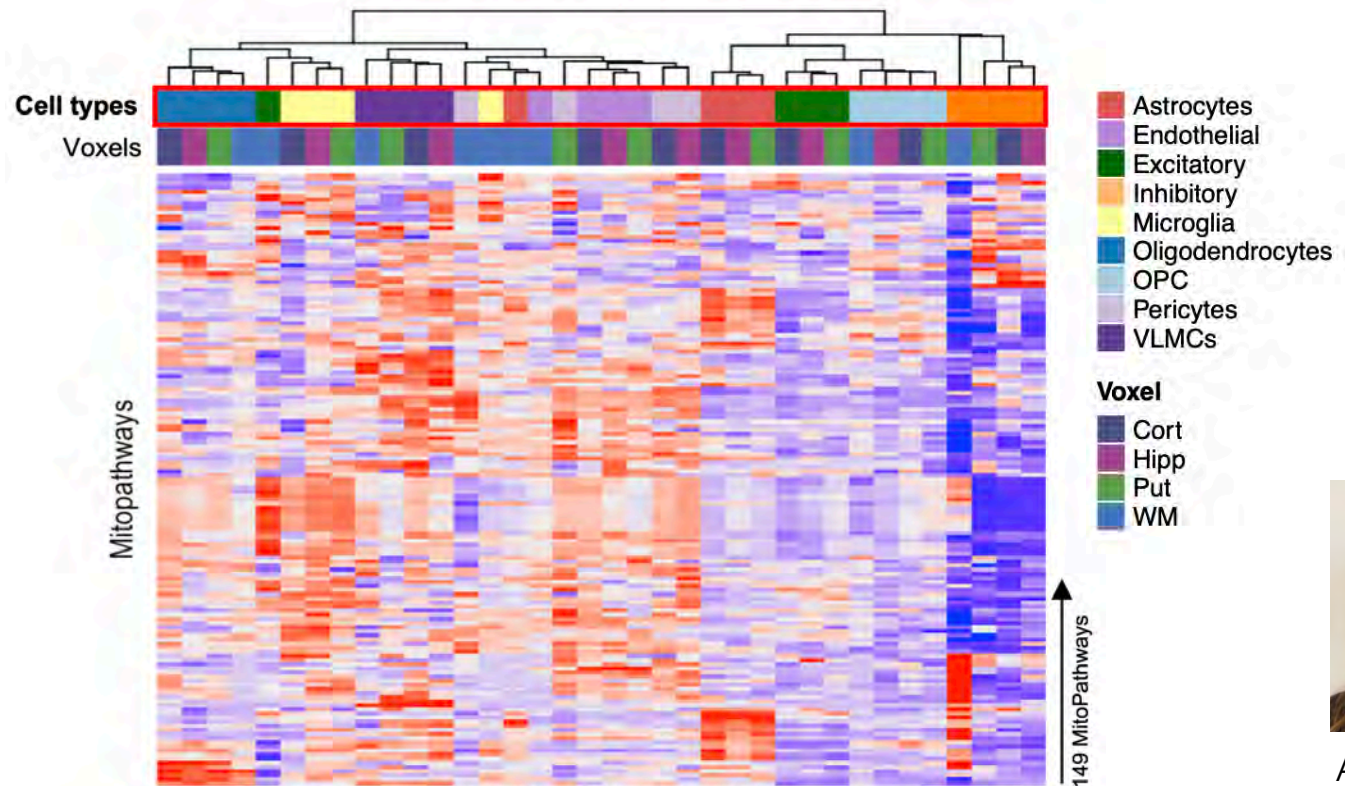




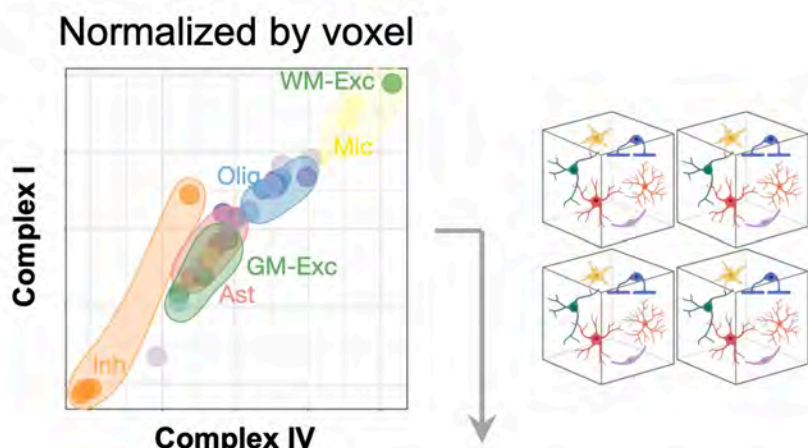
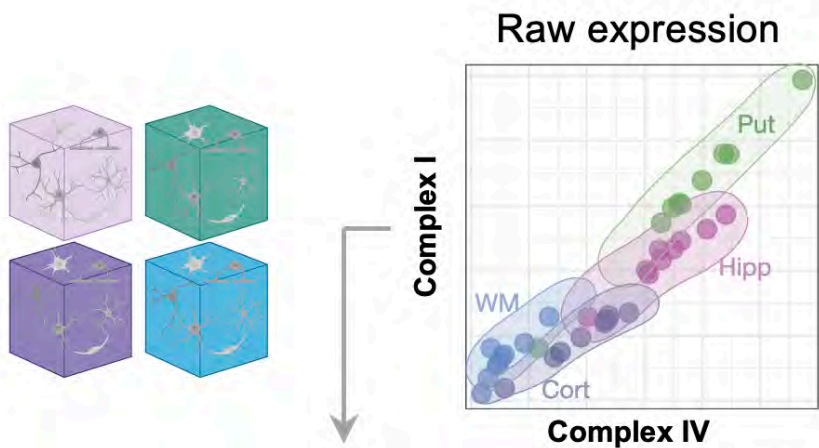
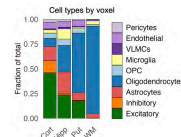
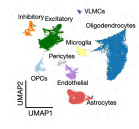
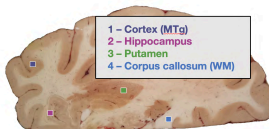
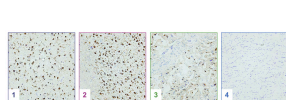
Normalized by voxel



Cell type-specific mitotypes

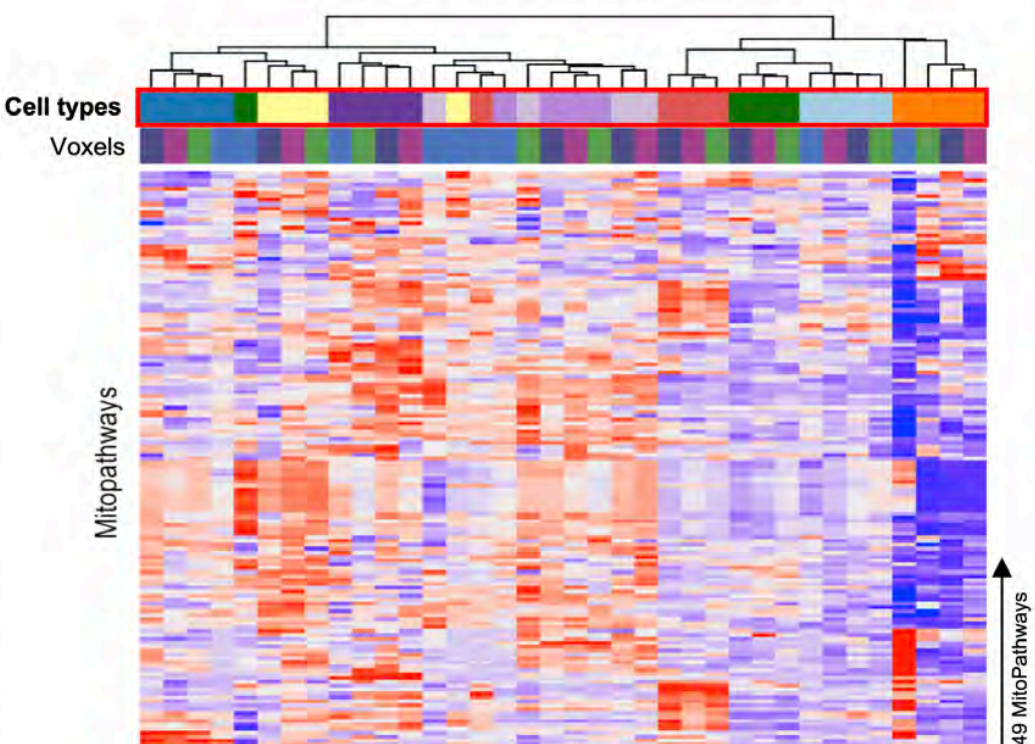
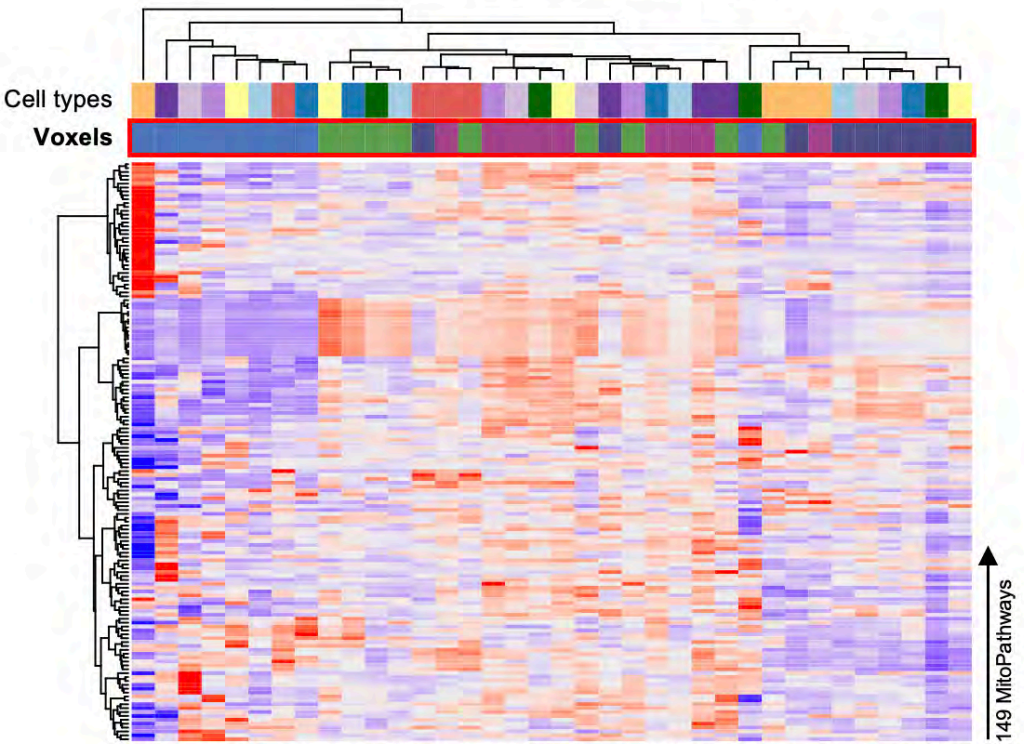


Anna Monzel



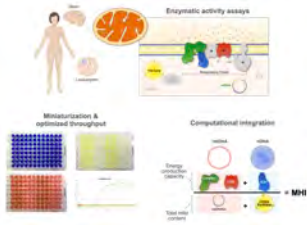
Voxels-specific mitotypes

Cell type-specific mitotypes

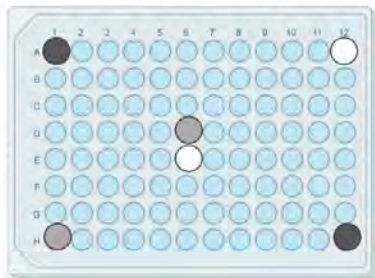


**Human brain mitochondrial specialization is driven by
both REGIONS & CELL TYPES**

OxPhos and mtDNA profiling



Assay plate layout



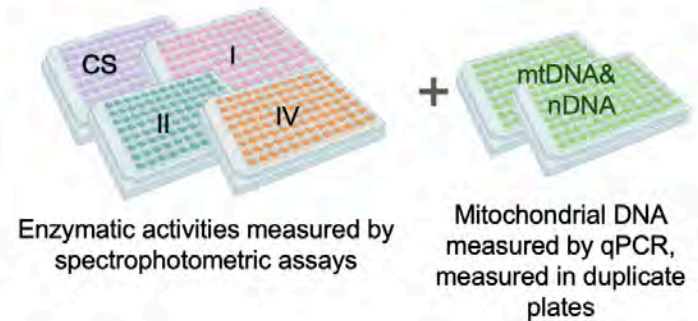
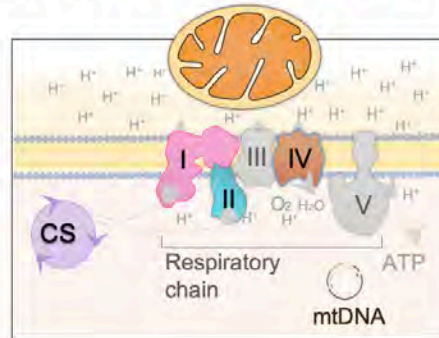
- Controls**
- Grey matter
 - White matter
 - Mixed tissue

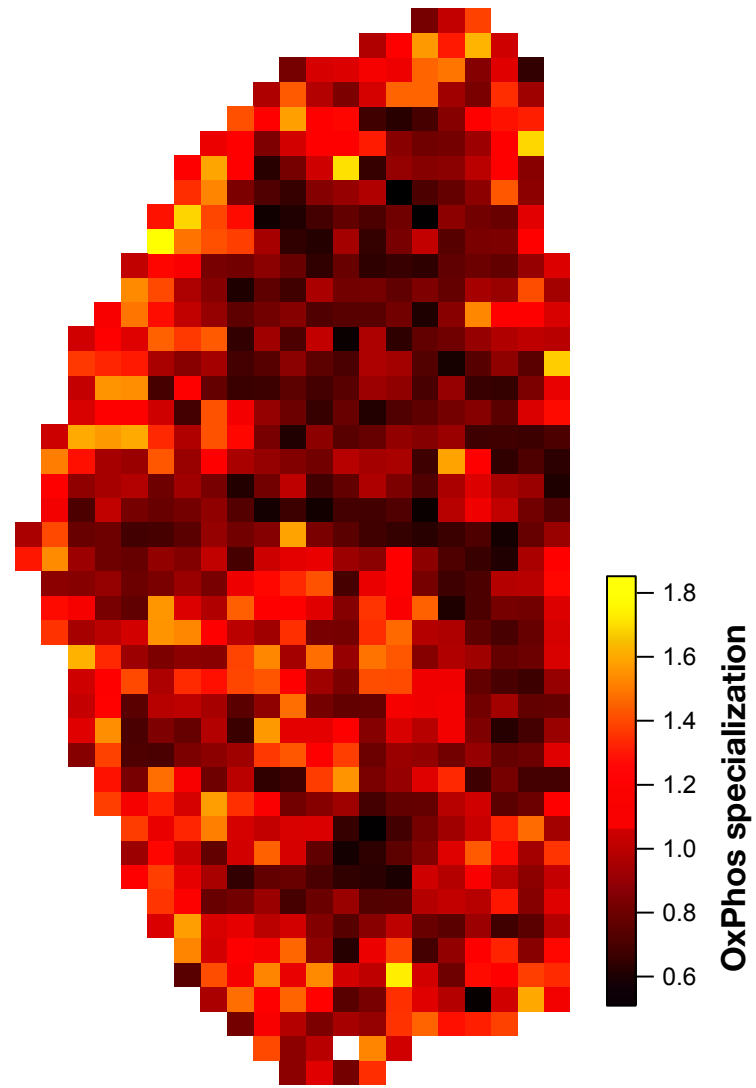
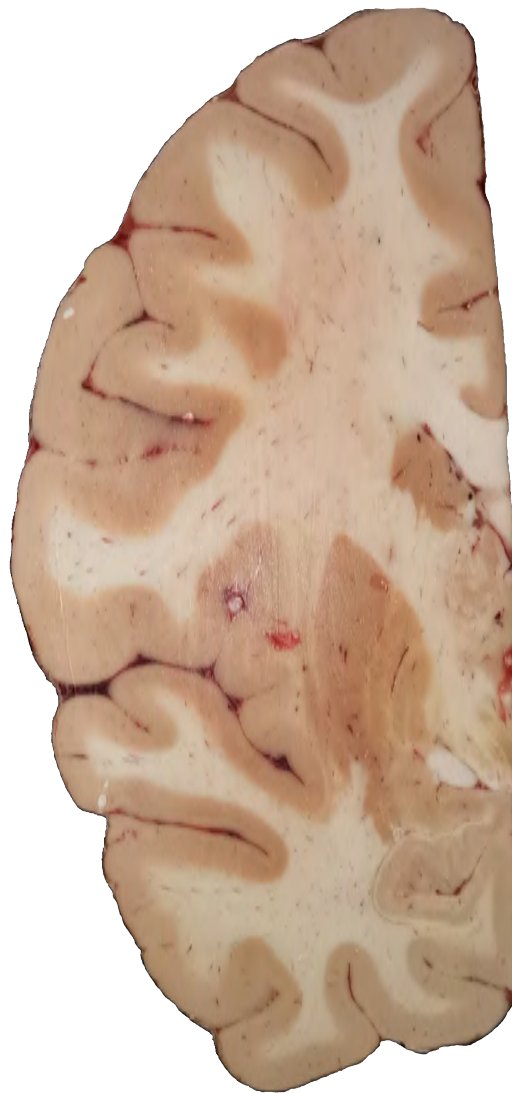
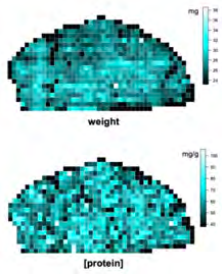
90 unique voxels per plate
8 plates total



3x triplicate negative control plates 3x triplicate plates

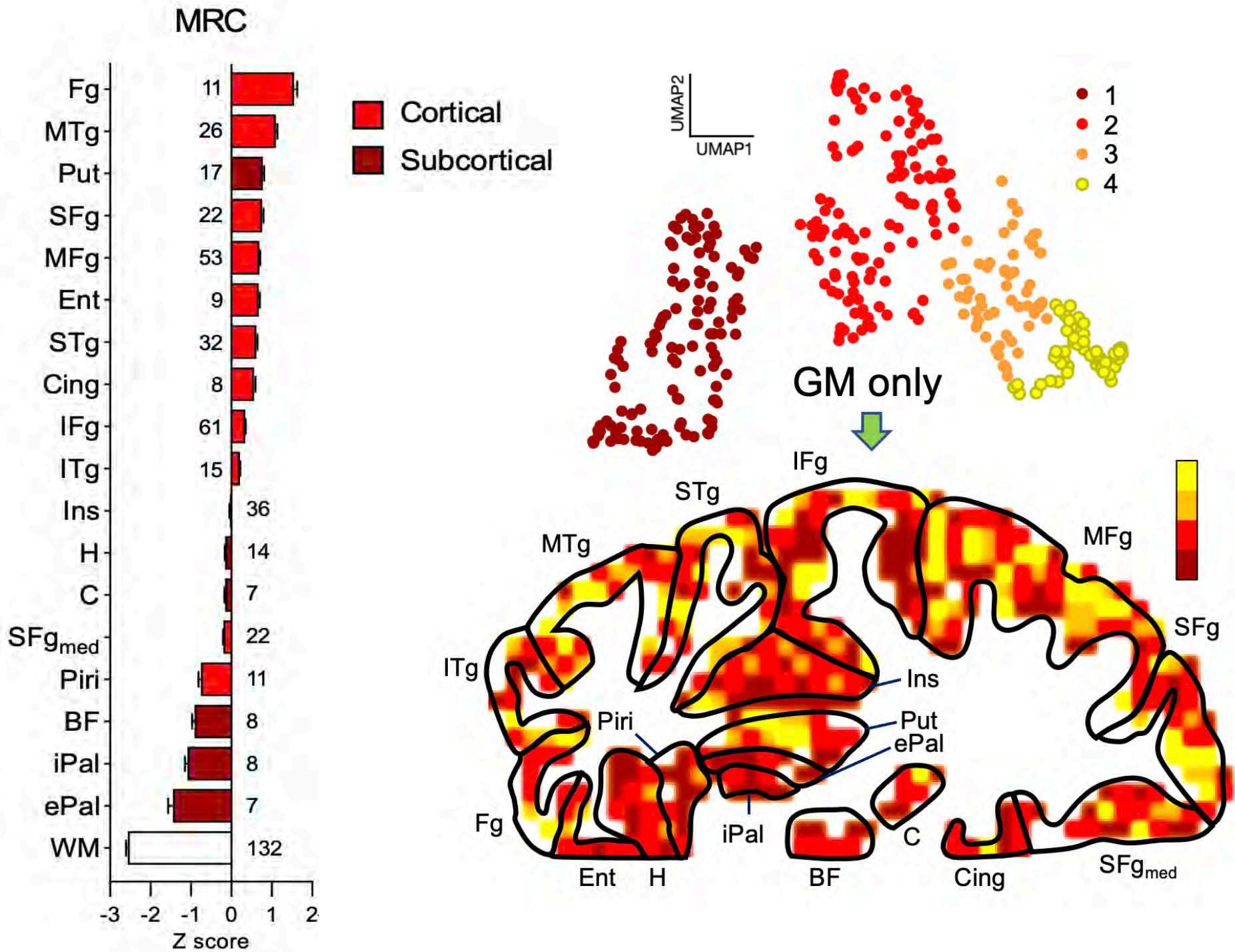
Mitochondrial colorimetric assays





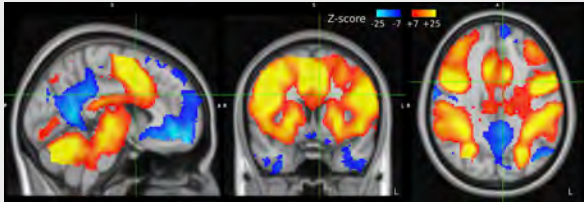
Mitochondrial profiling of 703 physical
brain voxels at fMRI resolution

Eugene Mosharov
Ayelet Rosenberg
Michel Thiebaut de Schotten

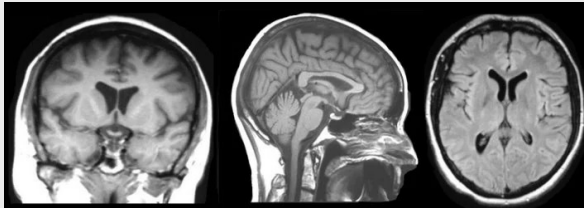


Building a predictive model of brain mitochondria

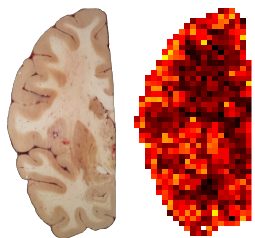
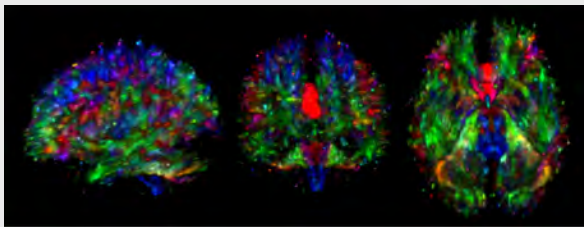
fMRI-BOLD



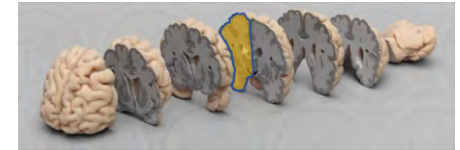
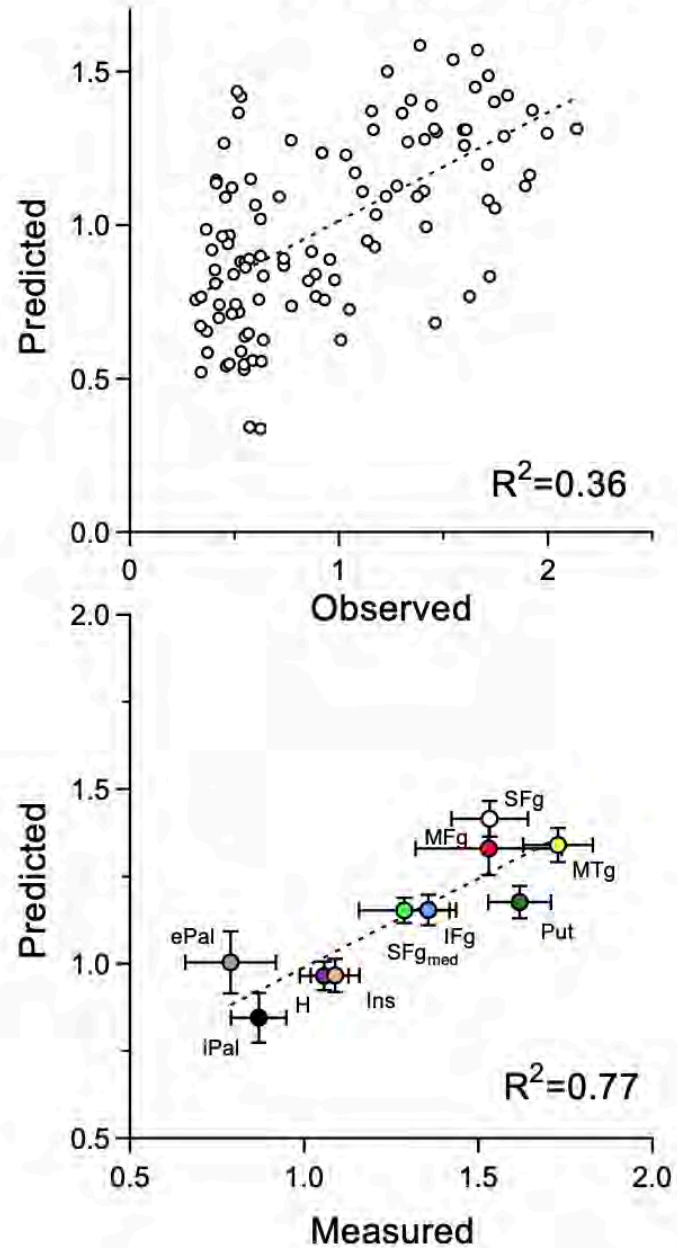
T1/T2 structural



Diffusion imaging



Training: 80%
Test: 20%



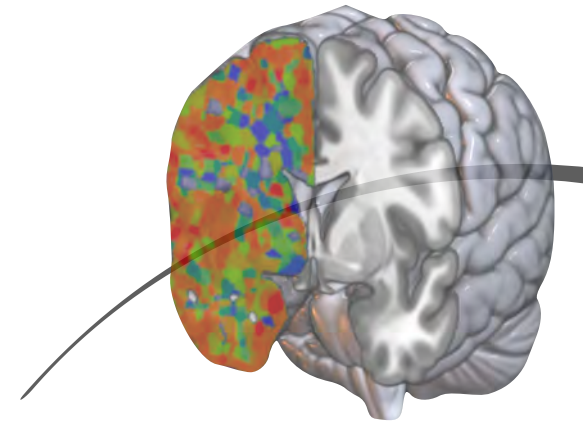
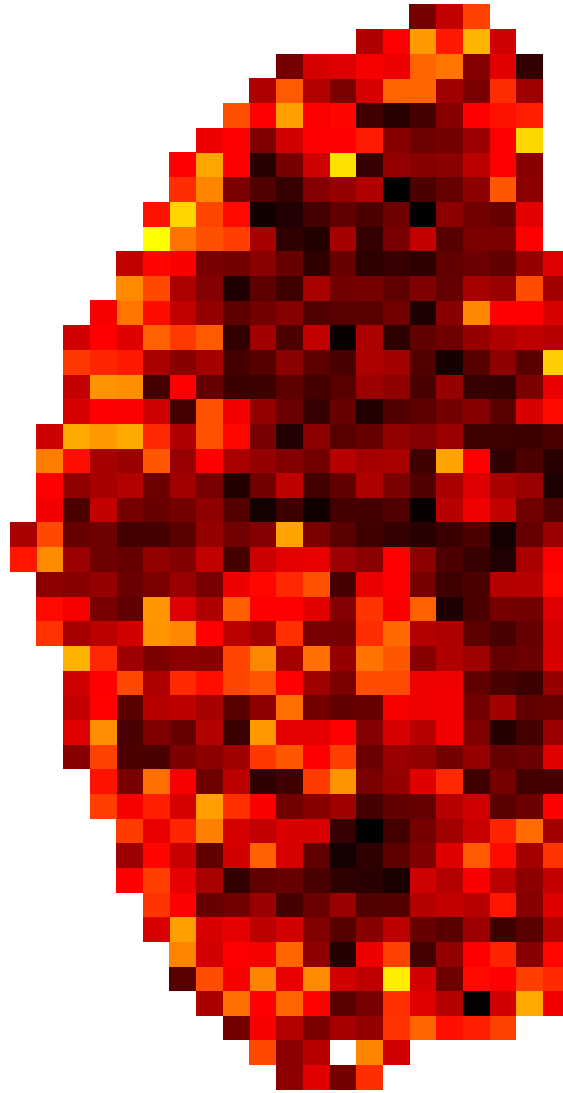
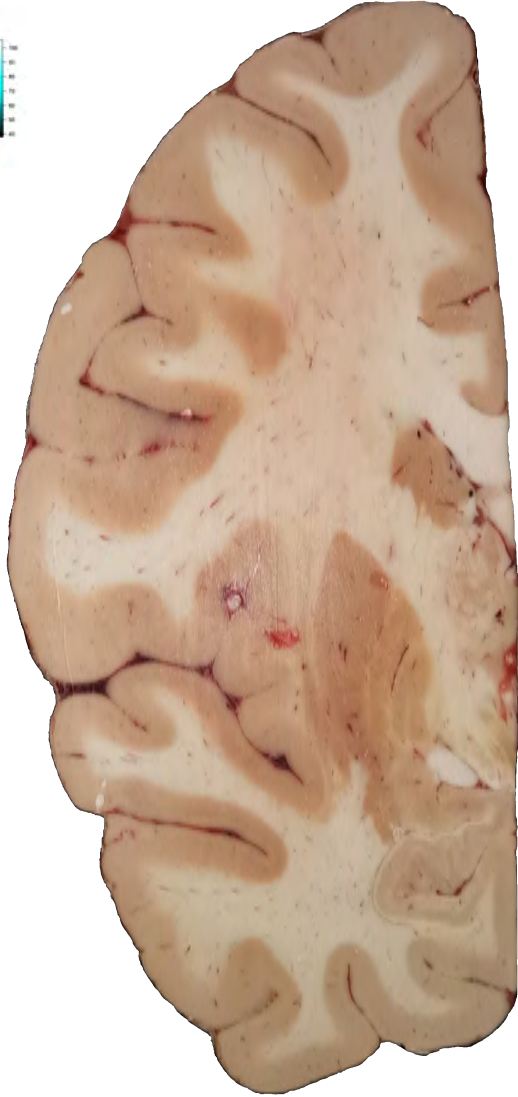
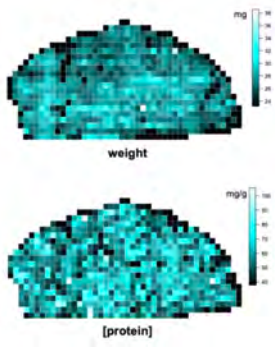
dorsal

medial

Occipital lobe (mean±s.d.)

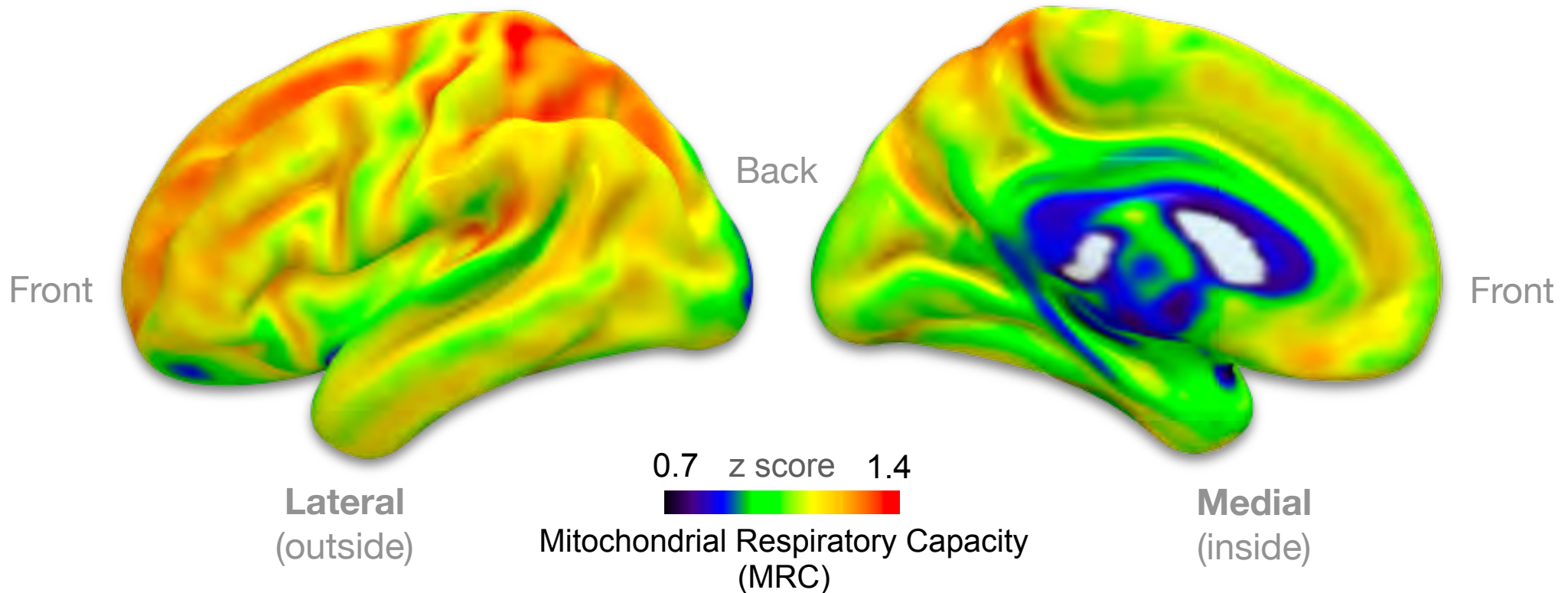
Feature	Observed	Predicted
CI	1.43±0.27	1.41±0.26
CII	1.25±0.16	1.35±0.14
CIV	1.44±0.17	1.31±0.24
MitoD	1.17±0.02	1.15±0.07
TRC	1.39±0.15	1.32±0.18
MRC	1.22±0.13	1.23±0.12

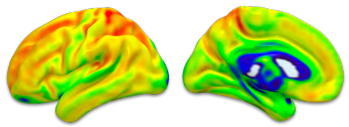
$r = 0.75$



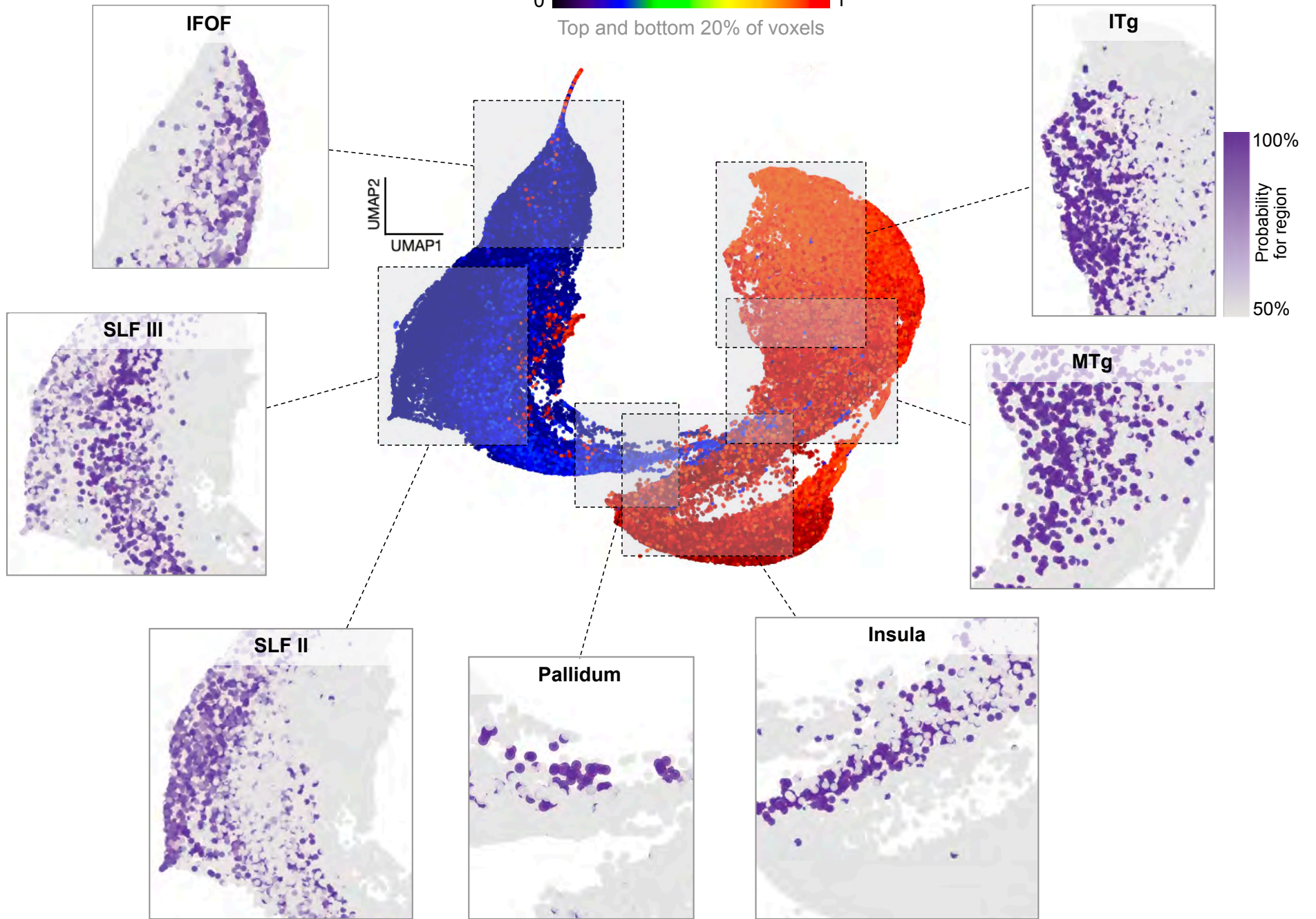
Mitochondrial profiling of 703 physical brain voxels at fMRI resolution

Back-projected onto 20 structural and functional neuroimaging modalities to create a probabilistic mitochondrial map across the whole brain (1.8M voxels)



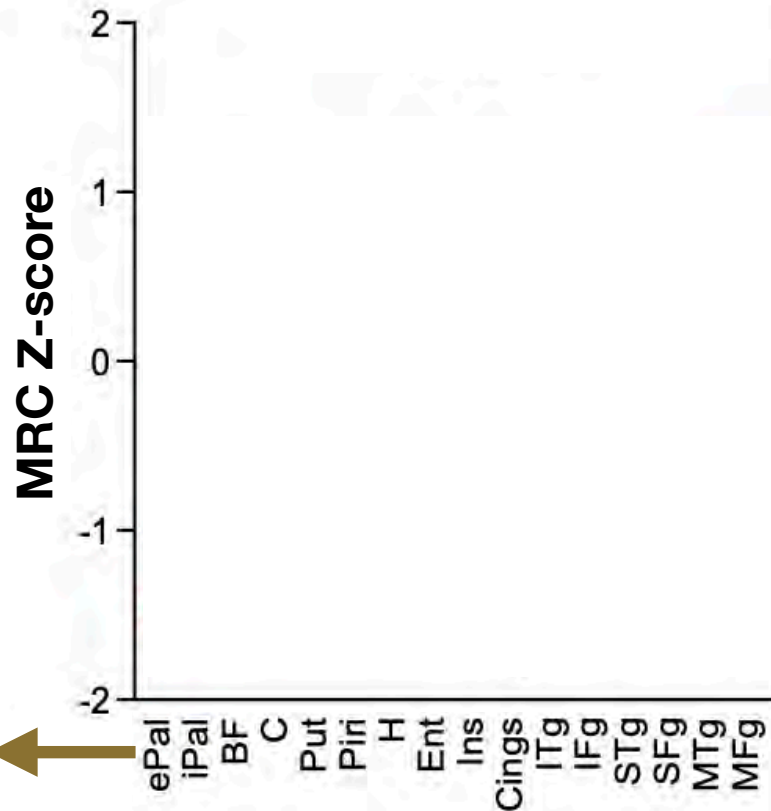


Grey matter probability
0 1
Top and bottom 20% of voxels



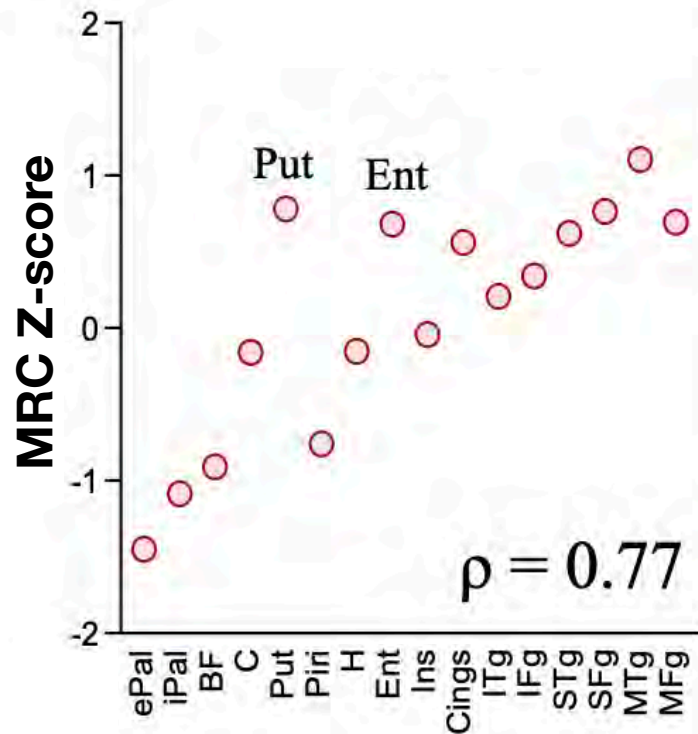
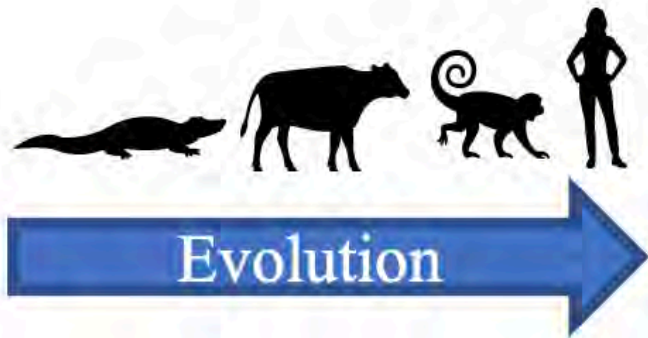
**Why are there different types of mitochondria
across the brain?**

Evolutionary correlate of mitochondrial OxPhos specialization

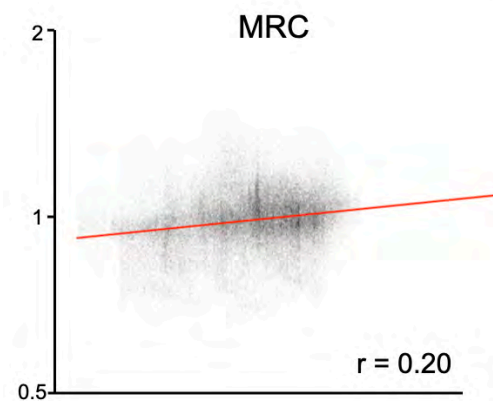
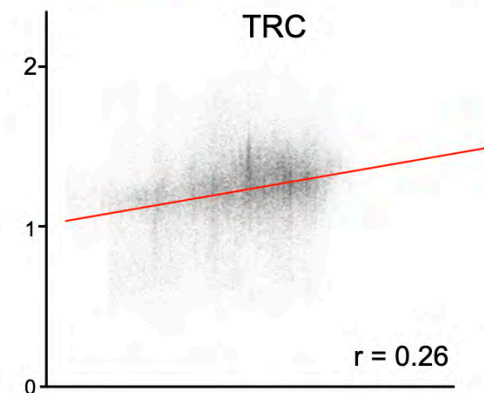
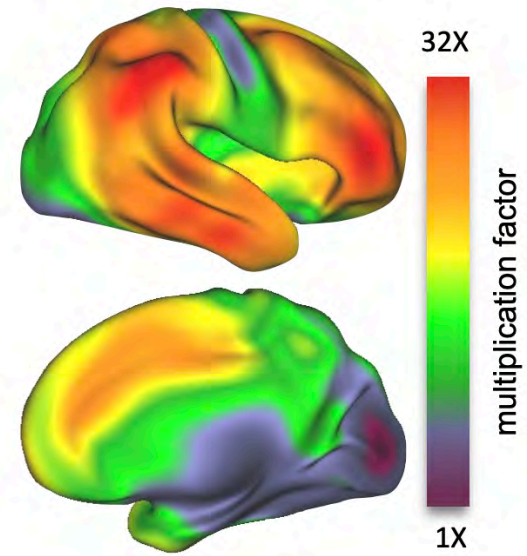


Most "ancient" ←

→ Most "recent"



Monkey to human expansion

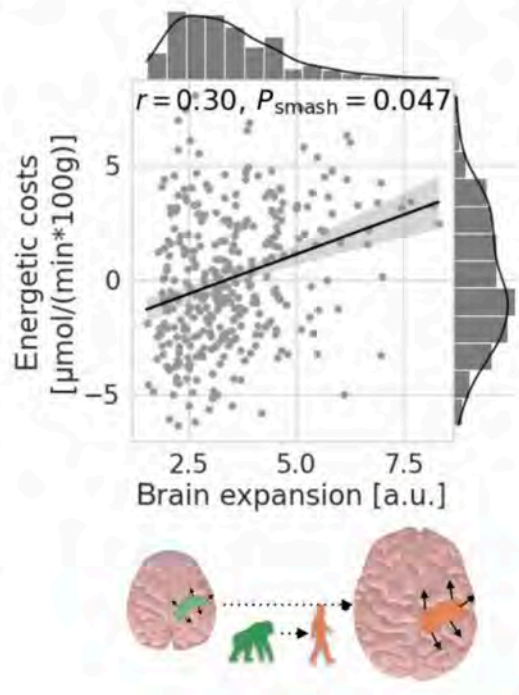


NEUROSCIENCE

An energy costly architecture of neuromodulators for human brain evolution and cognition

Gabriel Castrillon^{1,2,3}, Samira Epp^{1,4}, Antonia Bose^{1,4}, Laura Fraticelli^{1,4}, André Hechler^{1,4}, Roman Belenya^{1,4}, Andreas Ranft⁵, Igor Yakushev⁶, Lukas Utz¹, Lalith Sundar⁷, Josef P Rauschecker^{8,9}, Christine Preibisch^{1,10}, Katarzyna Kurcyus¹, Valentin Riedl^{1,3*}

B Human brain expansion

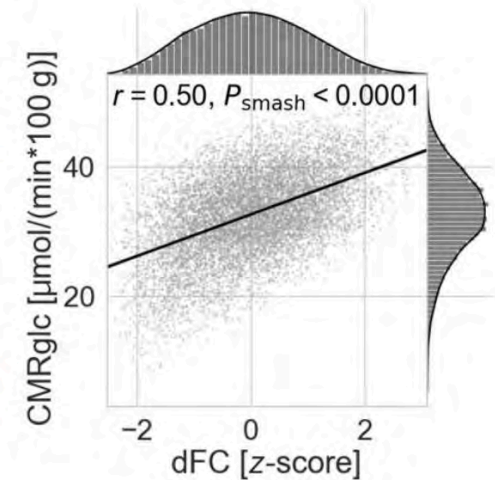
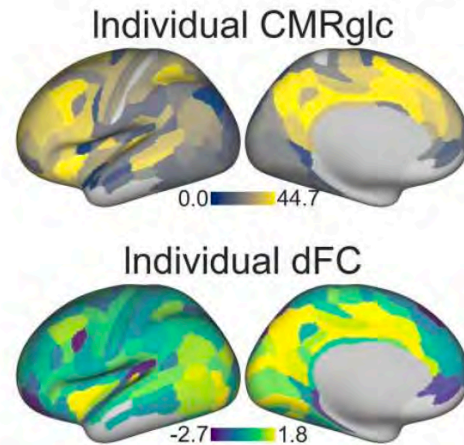


PET / MRI

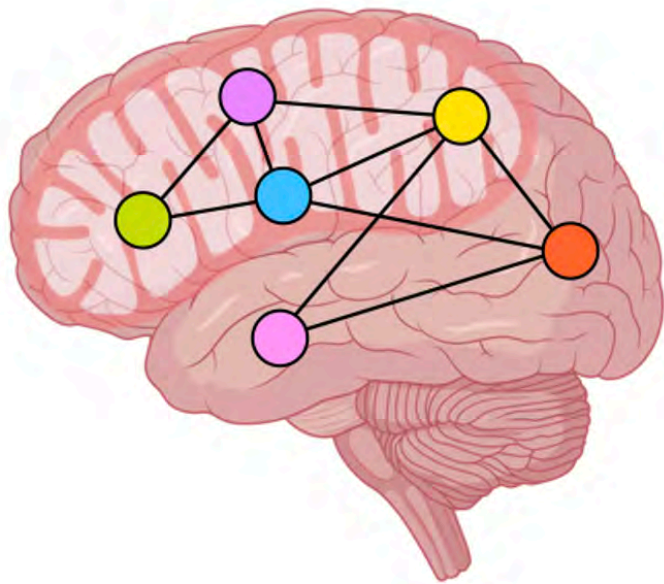


Arterial blood sampling

Subject space



G-coupled protein receptor expression correlates with glucose consumption

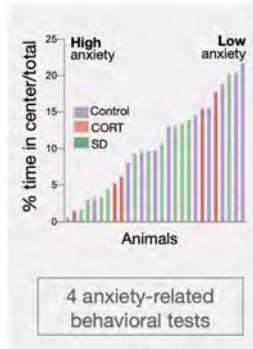
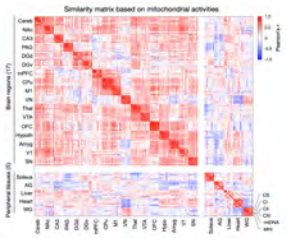
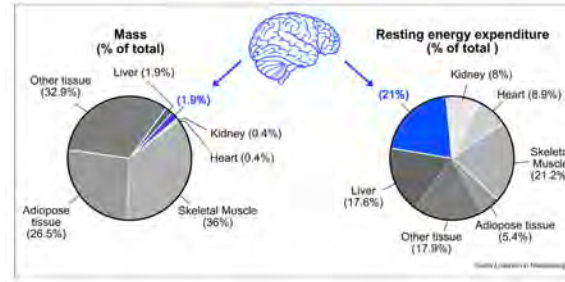
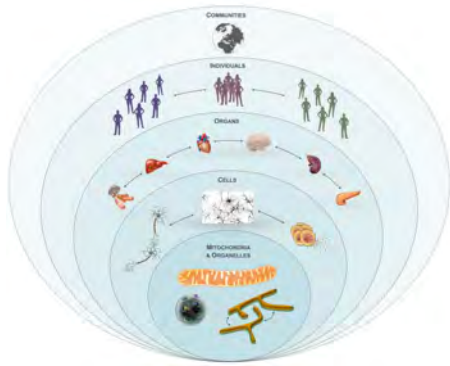


MITO BRAIN

ROSMAP



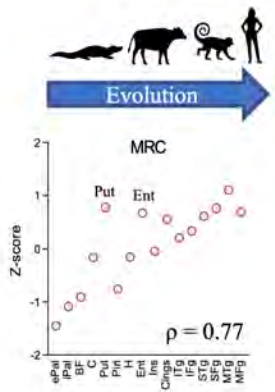
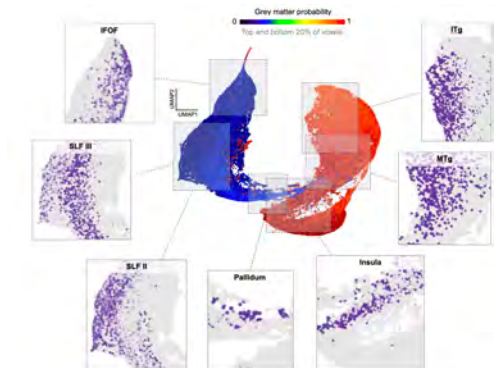
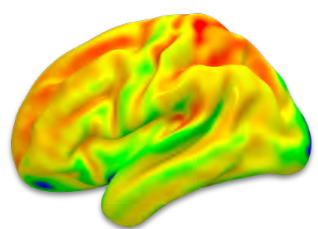
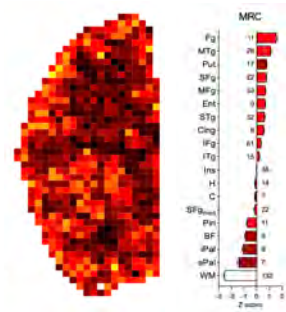
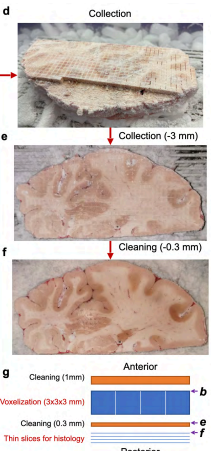
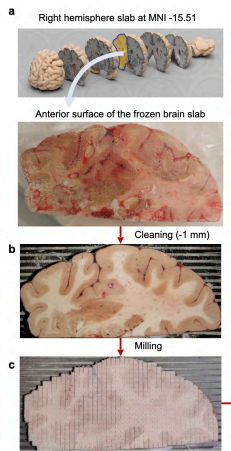
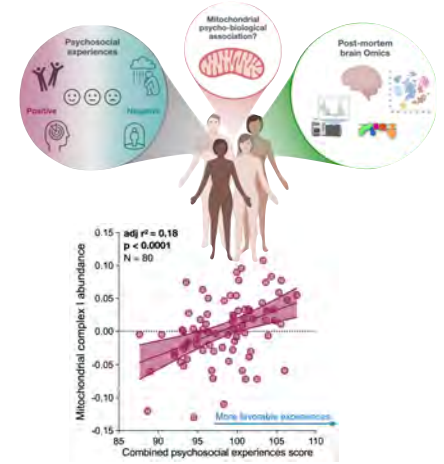
Cynthia Liu

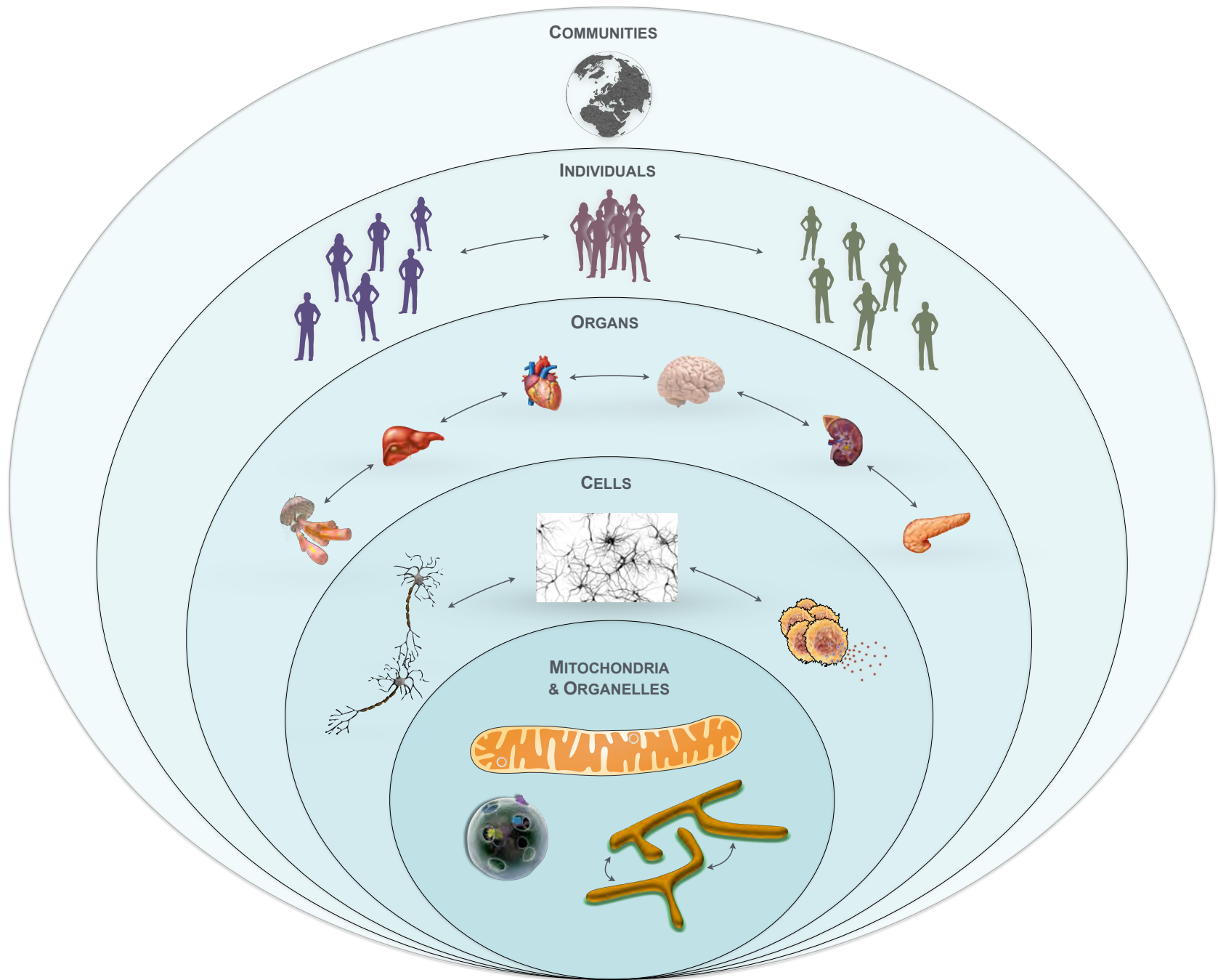


Network-based mito-behavior correlations

	OFT	EPM	NSF	SI
1	0.40*	0.74*	0.13	-0.69**
2	0.05	0.35	-0.45	-0.20
3	0.28	0.55	0.24	-0.09

Effect sizes (Pearson r) color scale: 0.5 (red), 0 (white), -0.5 (blue).

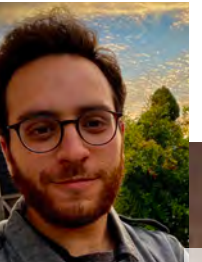




Mitochondrial PsychoBiology Lab

Linking molecular processes within mitochondria with the human experience

OUR RESEARCH



Ayelet

Eugene Mosharov (Sulzer Lab)

Caroline

Jack

Anna

Cynthia



Precious collaborators

Mitochondrial Biology & Medicine

Michio Hirano
Catarina Quinzii
CUIMC Neurology

Brett Kaufman
Pittsburgh University

Gyuri Hajnóczy
Erin Seifert
Thomas Jefferson University

● Orian Shirihai
Mike Irwin
UCLA

Tonio Enriquez
CNIC Madrid

Vamsi Mootha
Rohit Sharma
Harvard & MGH

Ryan Mills
University of Michigan

Gilles Gousspillou
UQAM

Jon Brestoff
Wash U

MiSBIE & MDEE Teams

Kris Engelstad
Catherine Kelly
Shufang Li
Anna Monzel
Janell Smith

Psychosocial Sciences

Robert-Paul Juster
Université de Montréal

Elissa Epel
Jue Lin
Aric Prather
Ashley Mason
UCSF

Eli Puterman
UBC

Clemens Kirshbaum
Dresden University

Anna Marsland
Rebecca Reed
Pittsburgh University

Suzanne Segerstrom
University of Kentucky

David Almeida
Penn State University

Energy expenditure & metabolism

Marie-Pierre St-Onge
Dympna Gallagher
Michael Rosenbaum
CUIMC Medicine

Chris Kempes
Santa Fe Institute

Herman Pontzer
Duke

Sam Urlacher
Baylor

Brain Neurobiology & Neuroimaging

● Phil De Jager
Hans Klein
● Vilas Melon
Stephanie Assuras
CUIMC Neurology

● Eugene Mosharov
● Dave Sulzer
● John Mann
● Maura Boldrini
● Mark Underwood
● Gorazd Rosoklija
● Andrew Dwork
● Chris Anacker
● Dani Dumitriu
Catherine Monk
Vincenzo Lauriola
Richard Sloan
Caroline Trumpff
CUIMC Psychiatry

Tor Wager
Dartmouth

● Michel Thiebaut de Schotten
CNRS Bordeaux

● Manish Saggar
Stanford

Anne Grunewald
University of Luxembourg

● Carmen Sandi
EPFL

Biological Aging

Steve Horvath
Morgan Levine
Altos

Albert Higgins-Chen
Yale

Marie-Abèle Bind
Harvard

Luigi Ferrucci
NIA Intramural

Dan Belsky
Linda Fried
CUIMC Mailman & Aging Center

BASZUCKI
BRAIN RESEARCH FUND

The Nathaniel Wharton Fund 

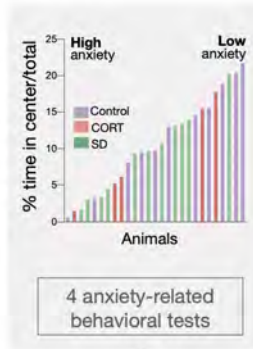
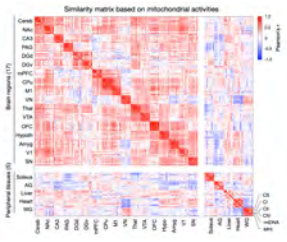
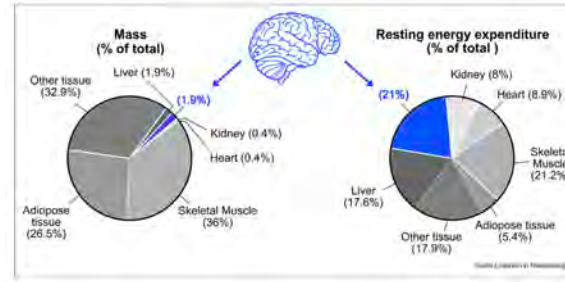
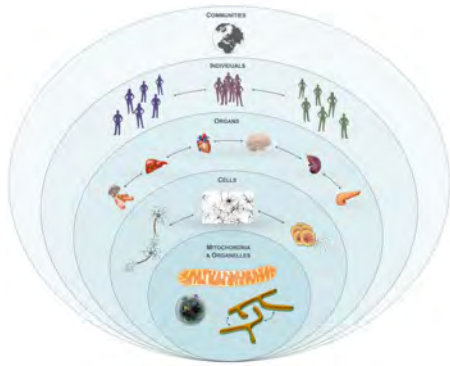
 National Institute of Mental Health

 National Institute of General Medical Sciences

 National Institute on Aging



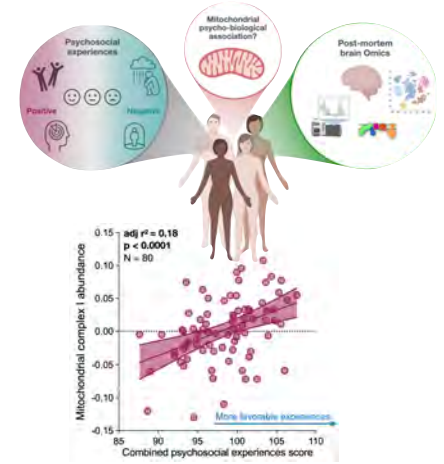
Downloadable
presentation slides



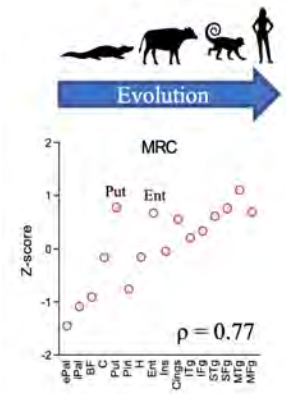
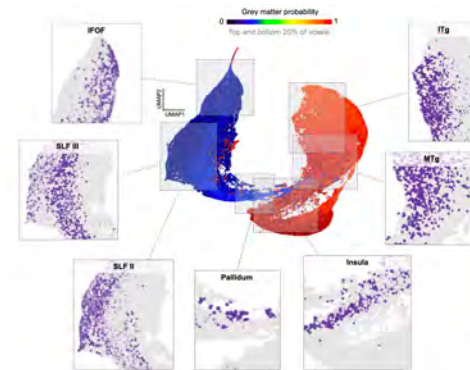
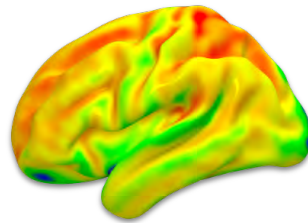
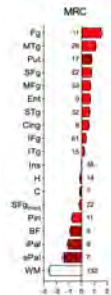
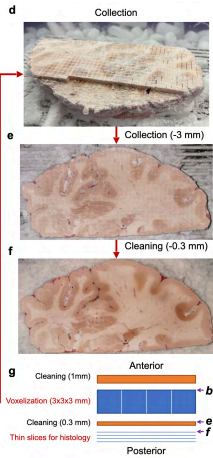
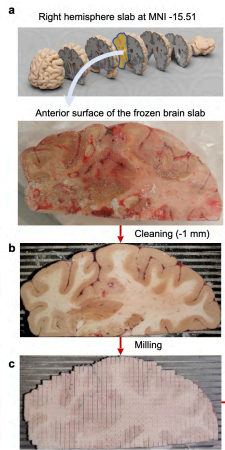
Network-based mito-behavior correlations

	OFT	EPM	NSF	SI
1	0.40*	0.74*	0.13	-0.69**
2	0.05	0.35	-0.45	-0.20
3	0.28	0.55	0.24	-0.09

Effect sizes (Pearson r) color scale: 0.5 (red), 0 (white), -0.5 (blue).



Correlations



Extended Data Table 1 | List of neuroimaging metrics and their standardized beta coefficient relationship with the mitochondrial features.

	Abbreviation	MRI metric	CI	CII	CIV	MitoD	TRC	MRC
Diffusion MRI	AD	axial water diffusivity		.242			.246	
	FA	white matter density			.681	.820		
	RD	radial water diffusivity	-.365		.439	.632		-.175
	StreDensity	streamlines density		-.184				
	ICVF	intra-cellular volume fraction	-.371					
	ISOCF	extra-cellular volume fraction		-.158	-.438	-.445	-.330	
	MD	mean water diffusivity						
	OD	orientation dispersion index (neurite complexity)	.363	.323	.628	.499	.481	.334
Structural MRI	T1W	T1w imaging						
	T2W	T2w imaging	-.245	-.304	-.458	-.410	-.330	-.244
	T1w/T2w	T1w/T2w ratio	-.656	-.580	-.723	-.622	-.617	-.593
	FLAIR	imaging approach to see the anatomy of the brain		-.221		-.339		
	CT	cortical thickness						
	inner_CSA	local surface for inner cortical ribbon						
	plial_CSA	local surface for outer cortical ribbon						
	GM	probability of gray matter	-1.038		-1.382		-1.177	-.939
	WM	probability of white matter	-1.082		-1.263	-.312	-1.040	-.906
Functional MRI	Max_activity	maximum bold derived from fMRI			.380		.333	.501
	Reho	regional homogeneity		.145		.135		
	Entropy	synaptic complexity derived from fMRI			-.386		-.365	-.560
	ALFF	amplitude of Low-Frequency Fluctuation						
	fALFF	ratio between low and and high frequency fluctuations						